# Bikini and Nearby Atolls

## Part 2. Oceanography (physical)

### Circulation Systems of Bikini and Rongelap Lagoons
### Adjustment of Bikini Atoll to Ocean Waves
### Sea Temperature in the Marshall Islands Area

GEOLOGICAL SURVEY PROFESSIONAL PAPER 260-B, C, D

# Bikini and Nearby Atolls

## Part 2. Oceanography (physical)

### Circulation Systems of Bikini and Rongelap Lagoons

*By* WILLIAM S. VON ARX

### Adjustment of Bikini Atoll to Ocean Waves

*By* WALTER H. MUNK *and* MARSTON C. SARGENT

### Sea Temperature in the Marshall Islands Area

*By* MARGARET K. ROBINSON

GEOLOGICAL SURVEY PROFESSIONAL PAPER 260-B, C, D

UNITED STATES GOVERNMENT PRINTING OFFICE, WASHINGTON : 1954

**UNITED STATES DEPARTMENT OF THE INTERIOR**

**Douglas McKay, *Secretary***

**GEOLOGICAL SURVEY**

**W. E. Wrather, *Director***

For sale by the Superintendent of Documents, U. S. Government Printing Office
Washington 25, D. C. - Price 75 cents (paper cover)

# CONTENTS

[Chapters B, C, and D of Professional Paper 260 comprise the first section of Part 2, Oceanography]

# Circulation Systems of Bikini and Rongelap Lagoons

*By* WILLIAM S. VON ARX

Bikini and Nearby Atolls, Marshall Islands

GEOLOGICAL SURVEY PROFESSIONAL PAPER 260–B

UNITED STATES GOVERNMENT PRINTING OFFICE, WASHINGTON : 1954

## CONTENTS



## ILLUSTRATIONS

# BIKINI AND NEARBY ATOLLS, MARSHALL ISLANDS

## CIRCULATION SYSTEMS OF BIKINI AND RONGELAP LAGOONS

By William S. von Arx

ABSTRACT

Four and one-half months early in 1946 were spent in the field at Bikini and Rongelap Atolls to study the circulation systems within the lagoons. Later, in the laboratory, synoptic studies were made of kinimatically similar models based on early field data. The results of these studies were then tested against further observations made in the field. It was found that both lagoons exhibited a primary circulation (overturning wind-driven circulation) and a secondary circulation (rotary circulation composed of two counter-rotating compartments). The direction of the primary circulation and the division between the counter-rotating compartments of the secondary circulation were always contained in a vertical plane having roughly the azimuth of the prevailing wind. The vigor of both circulations varied with the average wind strength taken over the previous 24 hours. Perturbations of the primary and secondary modes of circulation were produced by tides and waves and by the North Equatorial Current, which surrounds the atolls of the northern Marshall Islands group. Seasonal changes also were noted: the circulation of the winter months, when the northeast trade winds prevail, showed a marked stability and strength which was lacking in the summer season, when the atolls are on the edge of the belt of doldrums.

In addition to the qualitative synopsis of the circulations, numerical data are presented in tabular form which show the volumetric exchanges of water between the lagoons and the ocean. An estimate is made of the rates of refreshment and overturning of each lagoon. A chart of the values of horizontal diffusion in the surface plane is given for Bikini atoll.

### INVESTIGATION

The greater part of the field data for this study was accumulated at Bikini Atoll during 4½ months residence there. The data from Rongelap Atoll were gathered in only 6 days. These data are probably more representative than the period of observation suggests, for the work at Rogelap Atoll was executed by a relatively large force and planned in the light of both the experience gained and the techniques used at Bikini Atoll. Neverthelesss, it should be assumed that all generalizations and discussions of principle are based upon observations made at Bikini Atoll and that they apply only to Bikini unless specifically extended to include Rongelap Atoll.

Table 1 shows the dimensions of Bikini and Rongelap Lagoons. The relatively large size of these lagoons prevents synoptic observations of their circulations. Therefore, in addition to the field work, 2 months were spent in the laboratory to develop a technique whereby the observations made in the field could be reproduced in kinematically similar models. In these the circulations could be studied synoptically. Two models of Bikini Atoll were built on a scale of 1/100,000 and one of Rongelap on a scale of 1/150,000. These were placed separately in a flow tank and subjected to approximately scaled ocean current, wind, waves, and tide. The behavior of each model was adjusted to resemble its prototype at all the points observed in the field, and the resemblance was assumed to hold for all points in between. A total of about 60 stations, composed of more than 100 observations of the vertical profile of velocity and repeated profile measurements, was available for the Bikini models; 37 vertical profiles of velocity were available for the Rongelap model. Through study of these models and the field data, selection was made of the most probable circulation hypotheses.

Table 1.—*Comparative physical dimensions of Bikini and Rongelap Lagoons*

| Specification | Bikini | Rongelap |
|---|---|---|
| Approximate volume ..... cubic miles | 5.0 | 8.5 |
| Approximate area [1] ..... square miles | 192 | 305 |
| Total reef length [1] ..... miles | 57 | 80 |
| Length of reef, awash ..... do | 29 | 53 |
| Length of island strip ..... do | 13 | 18 |
| Width of passes and channels ..... do | 15 | 9 |
| Average depth of lagoon [1] ..... fathoms | 26 | 28 |
| Average depth over reefs, awash ..... do | ½ | ½ |

[1] Nugent, 1946, p. 748.

### OBSERVATIONS

Four sources of energy have been found to drive the circulation within Bikini and Rongelap Lagoons: wind, waves, tides, and the North Equatorial Current. Most of the water motion of the lagoons is produced by the stress of the wind on their surfaces. The exchange of lagoon water with that of the sea is accomplished in winter (the trade-wind season) by the action of tides and waves, in summer (the doldrum season) by tides and the North Equatorial Current. The change of agencies occurs with the seasonal migration of the northeast trade-wind belt, which moves northward in summer leaving the northern Marshall Islands for the most part becalmed in the doldrums. The effect of the

Note.—Contribution No. 421 of the Woods Hole Oceanographic Institution.

presence or absence of the trade winds is so marked that constant reference to them must be made to present the field data and circulation hypotheses intelligibly.

The effect of the active forces is determined as much by the solid physical structures of the atolls as by the forces themselves. Each lagoon is essentially a "lake in mid-ocean," cupped in a shallow saucer-like basin supported by a solitary mountain peak. From a remote vantage point southeast of the atolls they must appear somewhat as shown in figure 85. The atoll structures rise abruptly from the ocean floor, which in this region lies at a depth of about 2,000 fathoms. Between the atolls, and sometimes coalescent with them, are flat-topped "seamounts", which Hess (1946) has described and called "guyots." These fail to reach the surface by 600 or 700 fathoms. Both the guyots and atolls influence the flow of the North Equatorial Current and disturb its westward motion through the area. Waves and swells also progress westward through the atolls during the trade-wind season and pound continuously on the eastern and northern reefs. As a result of this pounding and the uneven supply of nutrient materials from the sea, the windward reefs, broadly speaking, are concave upward and impound water as shown in figure 86 while the leeward reefs are convex upward.

Along most of the length of the windward reefs there is a broad water-filled terrace fenced in by the island strip on the lagoon side and a cavernous bulwark of coral and algae on the seaward side, shown in section in figure 86.

The cavernous structure is honeycombed with rooms connected to the sea by surge channels (Tracey, Ladd, and Hoffmeister, 1948) and (Munk and Sargent, 1948). Cracks in the arches of the rooms are open to the sky. Swell rammed up the surge channels fills the rooms and forces water upward through the cracks and onto the terrace. The surface of the water on the terrace was measured repeatedly by H. J. Turner at a level approximately 0.5 meter higher than the level prevailing in the lagoon. In response to this steady head the terrace water flows between the islands into the lagoon. At Bikini atoll several hundred photographic measurements of the trails left by dye bombs dropped on the reef from aircraft, show an average inward velocity of flow of nearly 50 centimeters per second. The flow is continuous throughout the trade-wind season and supplies approximately one-third of the volume of new water added to the lagoon each day. During the doldrum season, when the ocean swell is much reduced, this inflow becomes negligible or even reversed.

Over the rounded leeward reefs similar aerial observations of the flow show that the water transport alternates with the tides. The leeward reefs are submerged so

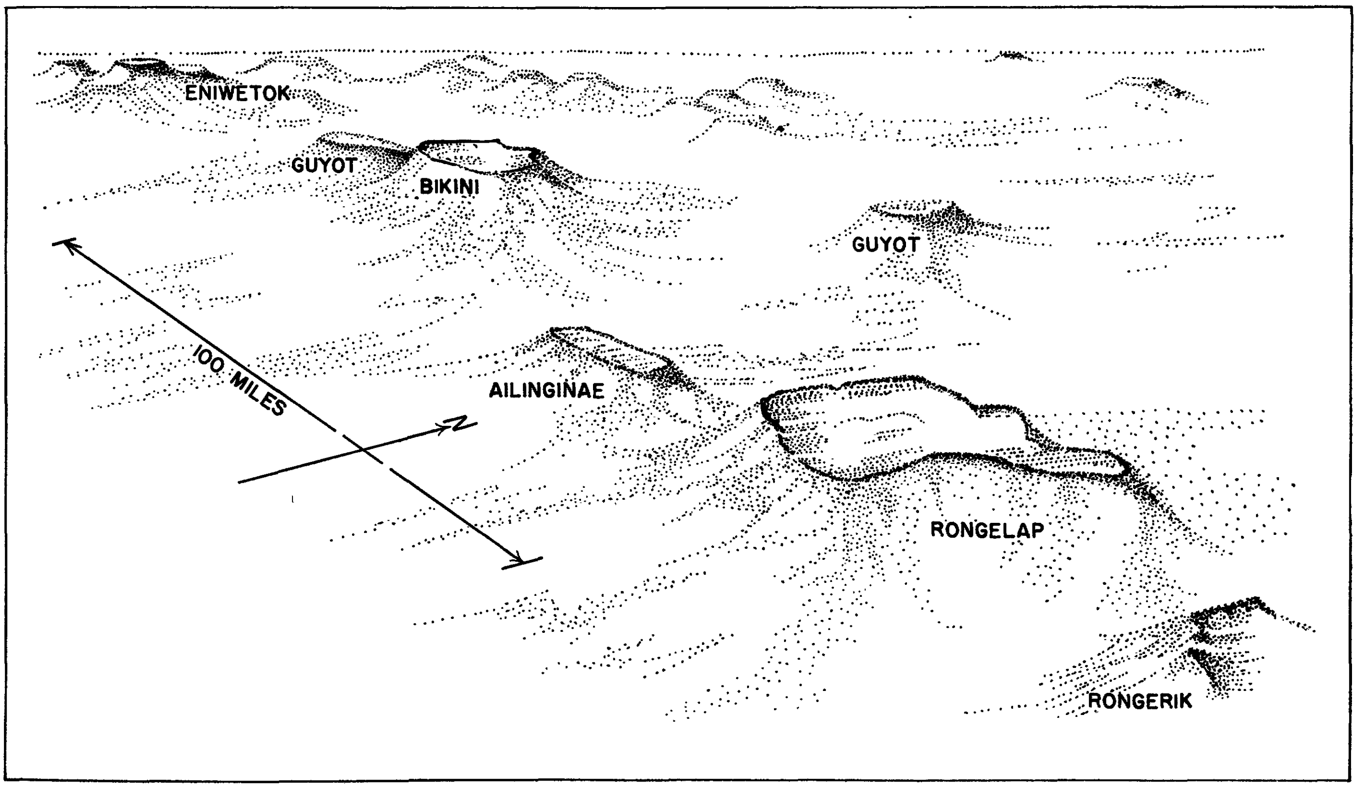


FIGURE 85.—Rongelap and Bikini Atolls and their surroundings, as they might appear from the southeast were the water removed.

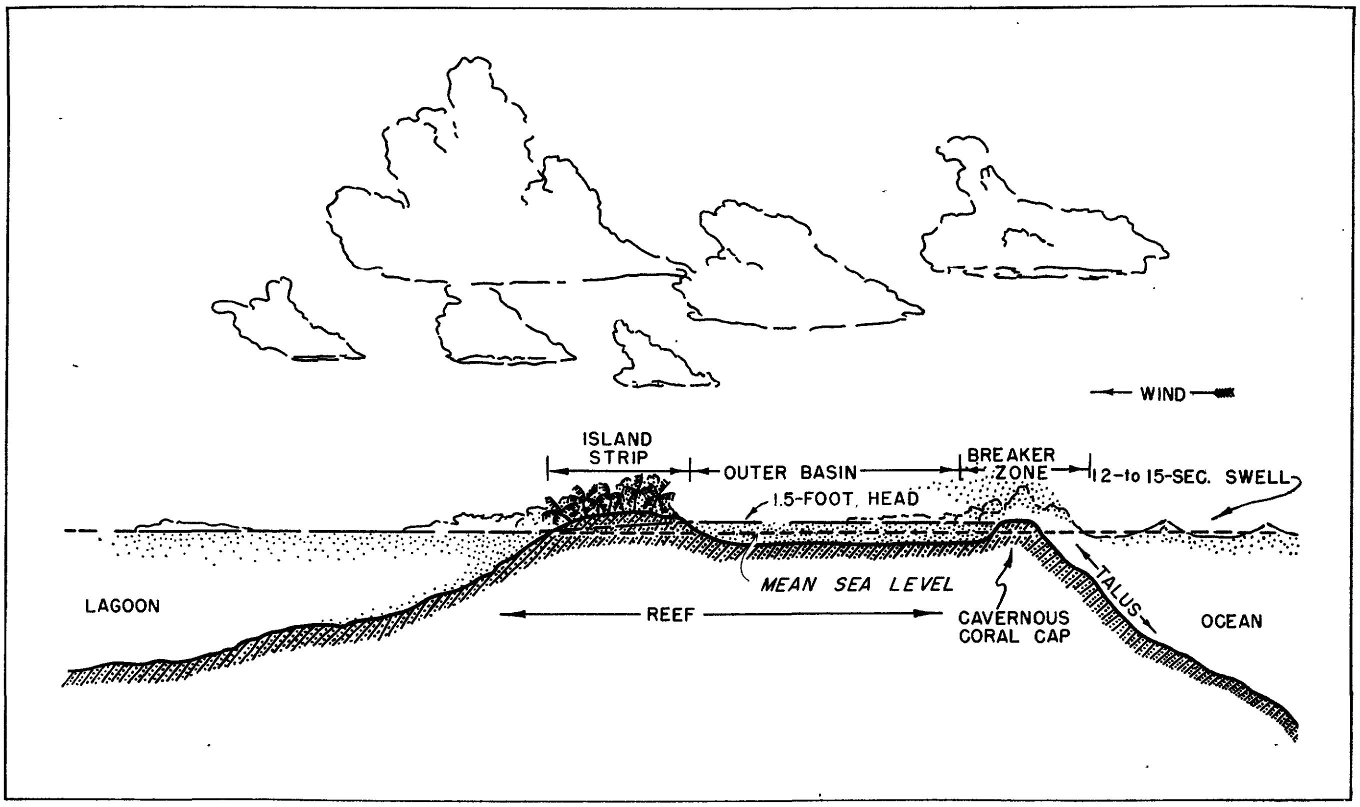


FIGURE 86.—Mechanism of continuous inflow across windward island strip.

that waves cross them, but since leeward waves are those which have been diffracted around the whole atoll, their energey is small and their approach oblique. The water driven by the wind along the surface of the lagoon toward the leeward reefs causes the flow over them to be predominantly seaward. During the doldrum season when the wind-driven surface current moves more slowly the tidal alternations of flow are more symmetrical.

The stress of the wind on the lagoon surface moves a layer of water along with it. More than 100 current measurements at 34 stations at Bikini Atoll show that the thickness of the surface layer changes with the strength of the wind from 5 to 20 meters and that its speed is very close to 3 percent of the average wind speed taken over the previous 12 hours. A characteristic thickness of the surface layer in winter is 13 meters and its average speed is 25 centimeters per second. In summer these values drop to an average thickness of 9 meters and a speed of less than 15 centimeters per second.

Throughout summer and winter in both lagoons the volume of water transported in the surface current is too great to be exhausted through the leeward passes or over the leeward reefs; consequently, some of the water sinks and returns upwind along the bottom as shown in figure 87. The bottom current is much thicker and slower than the surface current. It links the two ends of the surface current and produces a closed circulation which constitutes the primary overturning circulation system found in both lagoons.

The volume of water transported by the bottom current is somewhat greater than that carried by the surface current. When the bottom current reaches the lee of the windward reefs the water is forced upward. The greater portion finds its way back into the surface current, but a small fraction of the upwelling water diverges in the lee of the island of Bikini at Bikini Atoll and in the lee of Eniaetok (island) at Rongelap Atoll and flows in opposite directions along the reef. Measurements made at Bikini Atoll show the wind-driven surface layer to be less than 2 meters thick within 3,000 meters of the lee of islands along the windward reef, and within 2,200 meters in the lee of open reef. The fetch needed to produce a wind-driven surface current of normal thickness has been arbitrarily chosen as the width of the zone of upwelling. The divergent currents within this zone and their extensions along the reef constitute the secondary circulation system found in both lagoons.

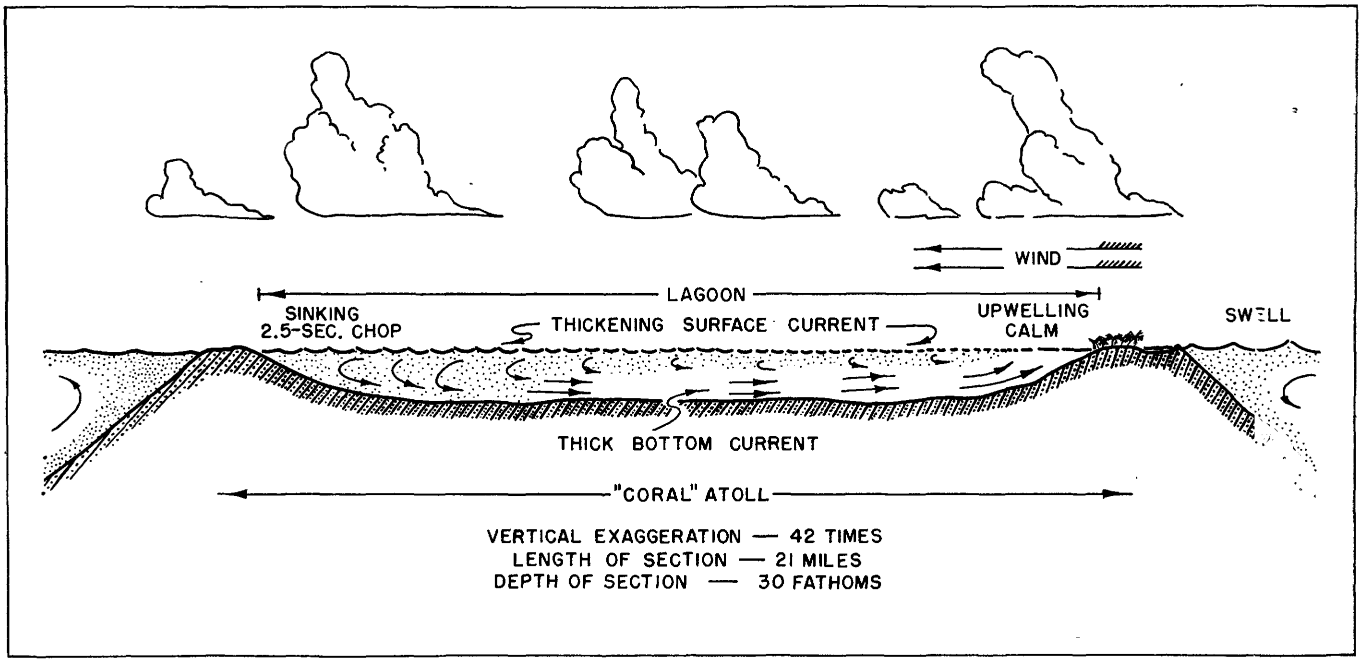


FIGURE 87.—Nature of wind-driven overturning circulation (schematic).

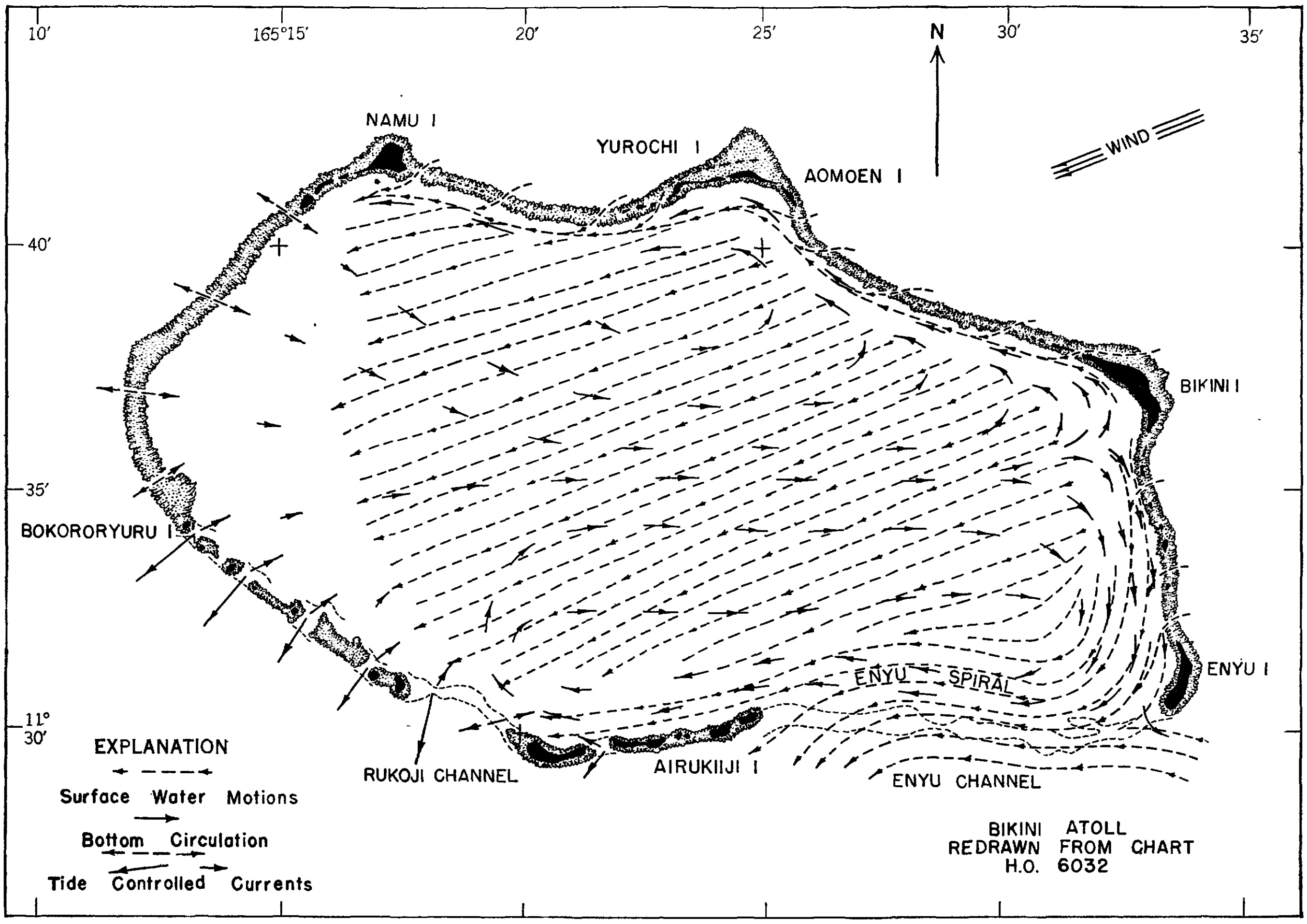


FIGURE 88.—Generalized circulation of Bikini Lagoon in winter.

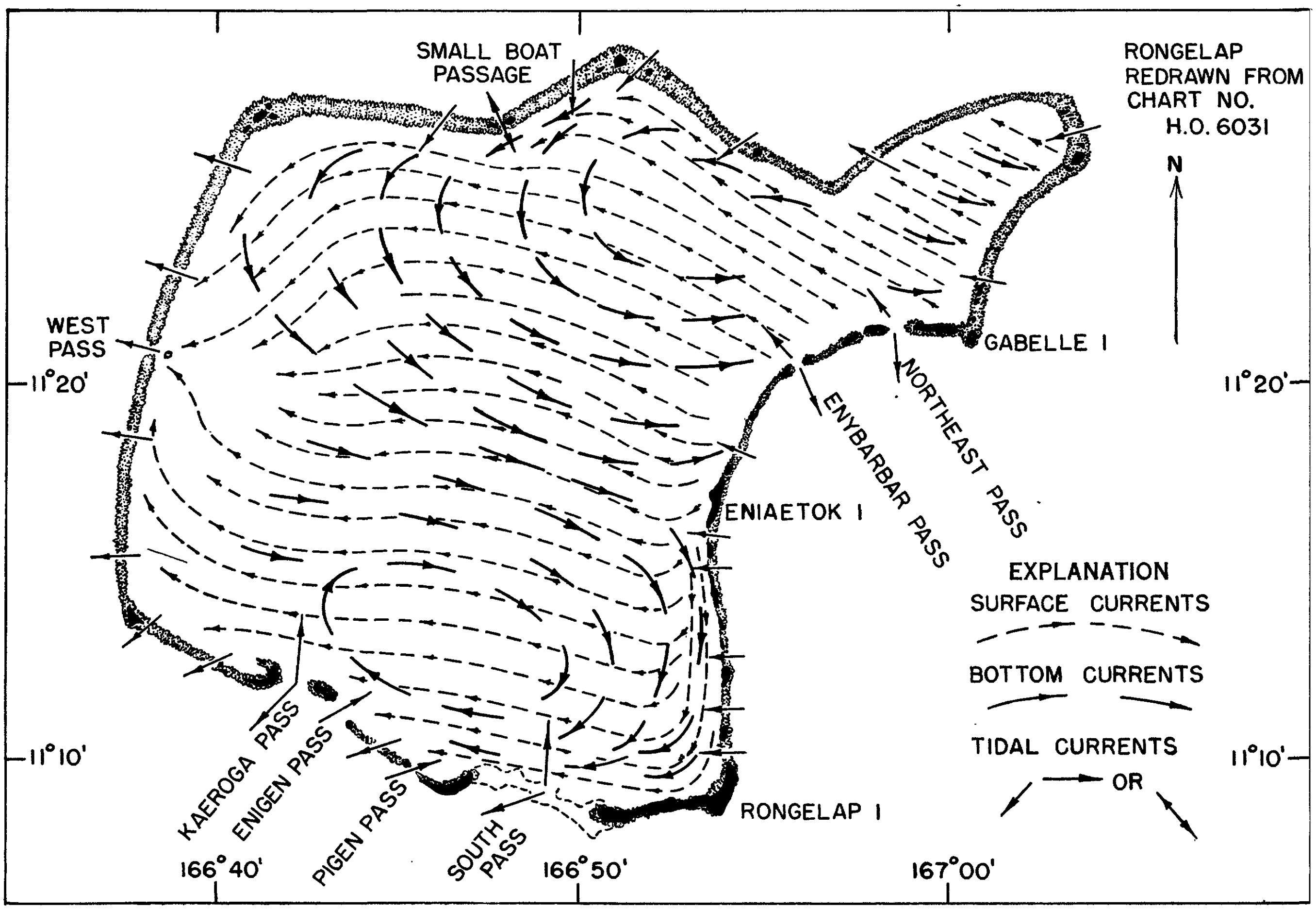


FIGURE 89.—Generalized circulation of Rongelap Lagoon under east-southeast winds.

The secondary circulation, shown in figures 88 and 89, divides the lagoons into two counter-rotating compartments, which move clockwise in the southern portions and counterclockwise in the northern portions. Beginning at the line of divergence in the lee of the windward reefs, a longshore current occuping the full depth of the lagoon basin can be traced along the reef in either direction. Both currents travel about half the lengths of the lagoons along the northern and southern reefs, respectively. Each longshore current is eventually confronted by a salient in the reef which turns the current into the body of the lagoon. At each of these points the current sinks and becomes part of the bottom current where it is indistinguishable from the primary circulation system. The vertical motions described are made plausible by the nearly complete homogeneity of the lagoon water during the winter (trade-wind) season. The water structure is moderately stable in the summer (doldrum) season, hence vertical motions are likely to be less important.

At Bikini Atoll where this mechanism was discovered, the southern branch of the longshore current crosses the mouth of Enyu Channel. Because the channel is only 14 meters deep the bottom current has little chance of access through it to the sea. A current of ocean water sweeps around Enyu island and enters the lagoon through the eastern third of Enyu Channel at a speed of 20 to 40 centimeters per second. The southbound longshore current heading for the same part of the channel at a speed of 15 centimeters per second is forced upward and westward by the bend of the reef in the lee of Enyu island where it encounters the incoming ocean water. The result of this is, hypothetically, the Enyu spiral, a slowly overturning stream of water moving westward along the southern reef and islands with a speed of 20 to 35 centimeters per second. The Enyu spiral extends from top to bottom of the lagoon and is about 3,000 meters wide. In crossing the mouth of Enyu Channel the upper layers of the current are bowed in and out with the changing tide. The stream is split against Airukiiji island, at the west end of Enyu Channel, with a small component escaping into the sea at a rate of 35 to 45 centimeters per second. The remainder skirts the intermediate islands and again encounters the reef at the sill of Rukoji Pass. Here the upper 10 meters of the stream goes out to sea, and the bottom portion is turned northward by the Rukoji sill, and eventually eastward by the primary circulation, to become part of the normal bottom current. This bottom current is gathered from the western third of the lagoon, but it is not until it is augmented by the remains of the Enyu spiral and its counterpart along the northern reefs, which joins the flow at a point halfway between Yurochi and Namu islands, that it assumes its full strength. The introduction of ocean water at the Enyu spiral produces water of lower salinity than that found elsewhere in the lagoon.

In summer the Enyu spiral probably ceases to exist, for under the influence of light southeasterly summer winds Enyu Channel becomes a strong source of incoming ocean water. This forces a reorganization of the secondary circulation system.

The flow through the southwest passes and channels is predominantly tidal. Despite the fact that these gaps in the reef are direct openings to the sea and tidal currents move through them at speeds sometimes approaching 150 centimeters per second, they produce but little effect upon the lagoon circulation and its refreshment rate. This is because the water entering the lagoon on the flood tide through a pass does not get far from the mouth of the pass before the tide changes and draws most of it out again. It is estimated that only 30 percent of the water entering a pass on the flood tide remains in the lagoon at the completion of the ebb tide. This remainder is the quantity which was moved away from the influence of the pass by the primary lagoon circulation. On the flood tide, currents radiating from the southwestern passes were detected 5,000 meters inside the lagoon, but not all the water moving in response to the flow in the passes comes through them; hence, the radius of direct refreshment around the passes is probably somewhat less than 5,000 meters.

The southwestern passes at Bikini Atoll were studied intensively both from the air and from shipboard. It was found that the flow through them was 40 percent stronger on the ebb tide than on the flood. This condition counteracts in part the continuous inflow of water over the windward reefs in winter and the inflow through Enyu Channel in summer. The current through the passes is hydraulically induced by the difference in level between the ocean and the lagoon. The ocean rises and falls as a simple harmonic oscillator, but the lagoon level, restricted by the limited capacity of the passes to transport the required volumes and the constant inflow of water over the windward reefs, cannot keep in step. The lagoon surface probably oscillates through a slightly smaller amplitude than the ocean surface and is somewhat out of phase in the vicinity of the passes. The turn of the current in the passes is 25 minutes later than high water in the ocean and 10 minutes later than low water in the ocean. The duration of slack water is less than 2 minutes.

The situation is even more marked at Rongelap Atoll because the proportion of lagoon volume to the cross-sectional area of passes is 3.5 times greater This results in a larger head of water between the inside and outside of the lagoon during the midstage flood and ebb tides, which causes the water to flow much farther into the lagoon and take the form of a jet. Observations of the flow through three of the passes and simultaneous measurements as much as 8,000 meters inside the lagoon along the jet showed the arrival of the flooding current. Model studies of the same phenomenon indicated the length of the incoming column of the largest jet from Kaeroga Pass to be 10,000 meters and water to be pushed ahead of the jet as far as 12,000 meters from the pass. It is expected that the Kaeroga jet returns to the sea on the ebb tide considerably less water than would retrace its course through a corresponding pass at Bikini Atoll. The circulation through South Pass is probably more nearly comparable with the passes at Bikini Atoll.

West Pass in the middle of the leeward reef at Rongelap Atoll (fig. 89) is unusual in that it is constantly outflowing. It is probably one of the principal exits for surface water driven by the wind toward the western side of the lagoon. Current poles as much as 5,000 meters on either side of this pass were drawn toward it and eventually passed through it. The current speed in the pass has been estimated at between 250 and 500 centimeters per second.

## THE EXCHANGE BUDGETS

Tables 2 to 5 summarize the quantitative results of the circulation studies and are based entirely upon field observations. Despite the abundance of data on the water motions in the lagoon derived from current-meter stations, current-pole runs, dye-drift experiments and dye-bomb runs, and from secondary evidence based on geologic and biologic data, there are a number of important parameters which have been evaluated by means of an inspired guess. These parameters are chiefly those needed to convert velocity data into transport data and involve estimates of the average depth of water over different reef sections, correction for the sinusoidal change of flow of tidal currents, a correction for the observed maximum current to average current through the channels (Sverdrup and others, 1942), and an assumed steady state during the winter months. These assumptions are evaluated as follows: Average depth of water over the reefs (winter), 100 centimeters; correction for flow in passes, $V_{avg}=0.75V_{max}$; and correction for sinusoidal tidal flow, $2/\pi$. A further distinction in tabulating the data is made for channels and

TABLE 2.—*Calculated flow into and out of Bikini Lagoon in the trade-wind season*

[Positive values denote inflow; negative values, outflow]

| Location | Length (kilometers) | Depth (meters) | Velocity (cm/sec) | | | | Volume (m³/sec) | | | |
|---|---|---|---|---|---|---|---|---|---|---|
| | | | Tide stage | | | | Tide stage | | | |
| | | | High | Ebb | Low | Flood | High | Ebb | Low | Flood |
| Reefs (island to island): | | | | | | | | | | |
| Bokobyaadaa to Namu | 0.5 | (1) | 20 | 10 | 10 | 25 | 130 | 40 | 20 | 100 |
| Namu to Yurochi | 8.4 | (1) | 40 | 40 | 30 | 45 | 4,350 | 2,700 | 750 | 3,020 |
| Aomoen to Bikini | 9.8 | (1) | 40 | 50 | 25 | 40 | 5,100 | 3,900 | 740 | 3,140 |
| Bikini to Enyu | 5.4 | (1) | 0 | 40 | 20 | 30 | 2,100 | 1,730 | 320 | 1,300 |
| Bokobyaadaa to West | 8.5 | (1) | 0 | −15 | 0 | 20 | 0 | −1,020 | 0 | 1,360 |
| West to Bokororyuru | 6.3 | (1) | −5 | −5 | 5 | 5 | −410 | −250 | 90 | 250 |
| Total | | | | | | | 11,270 | 7,100 | 1,920 | 9,170 |
| Passes: | | | | | | | | | | |
| Rukoji Pass [2] | 3.5 | 8.7 | −5 | −15 | −5 | 45 | −1,500 | −4,500 | −1,500 | 13,700 |
| Enyu Channel | 15.7 | 12.2 | −2.5 | −3.0 | −2.5 | −2.0 | −4,800 | −5,800 | −4,800 | −3,800 |
| Total | | | | | | | −6,300 | −10,300 | −6,300 | 9,900 |
| Channels: | | | | | | | | | | |
| All southwest | 2.0 | 29.4 | −10 | −100 | −15 | 50 | −5,900 | −59,000 | −8,900 | 29,400 |
| Rukoji Pass [2] | .6 | 36.6 | −5 | −25 | −5 | 50 | −1,100 | −5,500 | −1,100 | 11,000 |
| Enirik Pass | .4 | 55.0 | −5 | −25 | −5 | 35 | −1,100 | −5,500 | −1,100 | 7,700 |
| Total | | | | | | | −8,100 | −70,000 | −11,100 | 48,100 |
| Corrected total for passes | | | | | | | −6,100 | −33,400 | −8,300 | 22,900 |

[1] Varies with stage of tide.
[2] Rukoji Pass, a "composite pass," is subdivided into its component parts.

passes. Passes are broad shallow openings in the reef for which $V_{max}$ and $V_{avg}$ are substantially the same; channels are narrow V-shaped openings in which bottom and side friction have important effects upon the measured maximum and average rates of flow. For this reason distinctions are made between passes and channels, and where composite features exist, as in Rukoji Pass, which has a channellike notch in its sill, the flows through the pass and channel portions have been separated.

Tables 2, 3, and 4 present data used in computing the volume of water involved in a tidal cycle during the trade-wind season and show that the volume is approximately $1.06 \times 10^9$ cubic meters. The total volume of Bikini Lagoon is approximately $28 \times 10^9$ cubic meters. Thus, 3.8 percent of the lagoon's volume is transported into and out of the lagoon per tidal cycle. Using this rate it requires about 13 days for the lagoon to exchange its own volume with the sea.

TABLE 3.—*Tidal transport of water per tidal cycle at Bikini Atoll, in trade-wind season*

[Net inflow, 786,000,000 cubic meters per day; net outflow, 792,000,000 cubic meters per day. Positive values denote inflow; negative values, outflow]

| Tide stage | Duration per cycle (hours) | Flow, in millions of cubic meters— | | | |
|---|---|---|---|---|---|
| | | Over reefs | Through passes | Through channels | Total |
| High | 0.5 | 21<br>−1 | −12 | −11 | −3 |
| Ebb | 5.8 | 175<br>−28 | −215 | −697 | −765 |
| Low | .5 | 3 | −12 | −15 | −24 |
| Flood | 5.2 | 172 | 256<br>−71 | 429 | 786 |

TABLE 4.—*Total transport of water in millions of cubic meters per tidal cycle at Bikini Atoll, in trade-wind season*

| Location | Flow, in millions of cubic meters— | |
|---|---|---|
| | Inflow | Outflow |
| Reefs | 21<br>175<br>3<br>172 | 1<br>28 |
| Passes | 256 | 12<br>215<br>12<br>71 |
| Channels | 429 | 11<br>697<br>15 |
| Total | 1,056 | 1,062 |

This, however, tacitly assumes that every particle of incoming water is retained in the lagoon and every particle of water exhausted is lagoon water, which is inexact if only to the extent that the passes exhaust on the ebb tide about 70 percent of the ocean water introduced on the previous flood. Thus, the rate of exchange should be reduced by an amount which is proportional to the ratio of the rate of exchange through the passes to that of the "rectified flow" over the reefs. This yields a correction factor of about 3.0, making a more reliable estimated rate of exchange with the open ocean of 1 lagoon volume in 39 days. This approximate value is valid only during the trade-wind season when a steady state can be assumed. Throughout the summer season no prolonged steady state exists, but it was found that the flow through the passes is reduced 50 percent and that over the reefs nearly 80 percent. The change in average wind direction from easterly to southerly occasionally forces water out of the lagoon

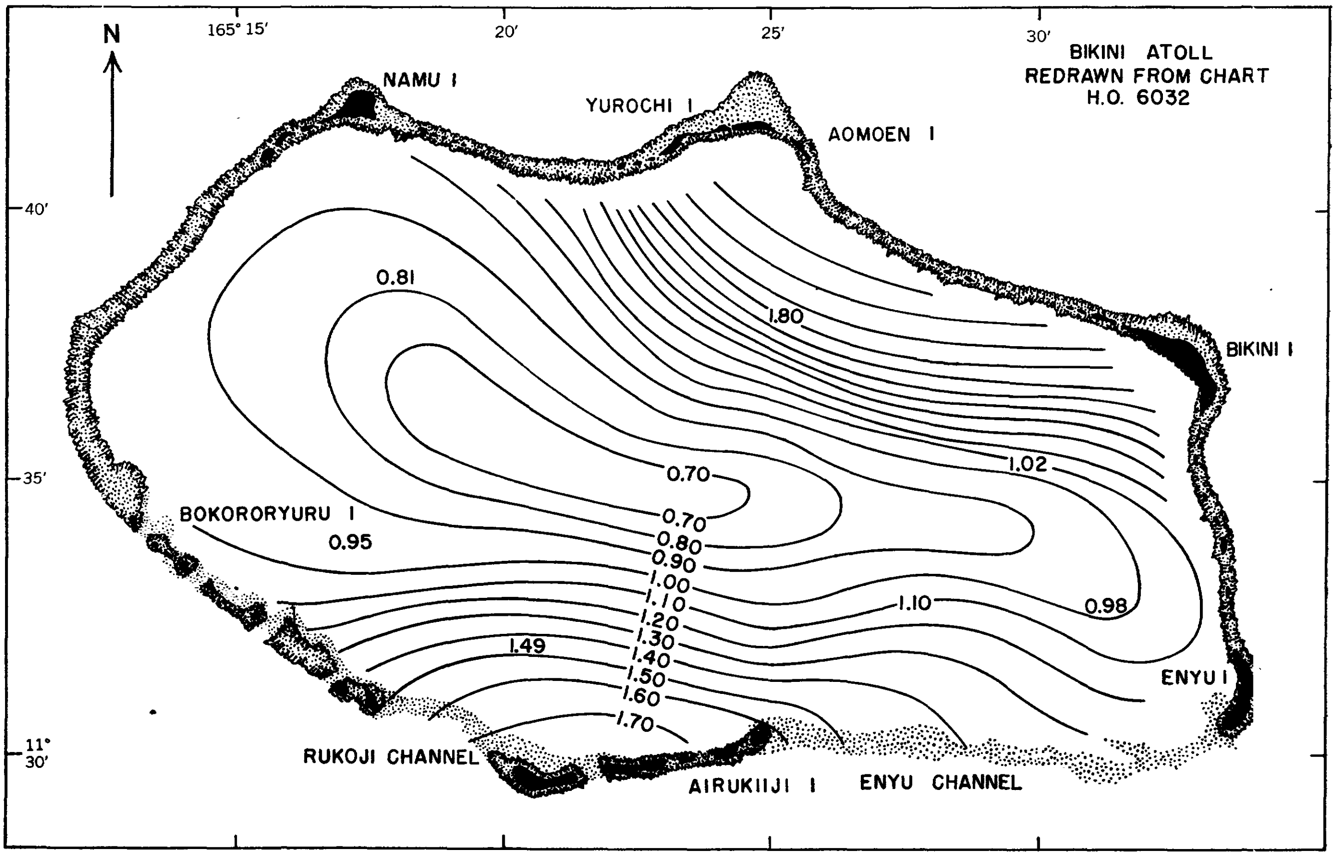


FIGURE 90.—Horizontal-diffusion rates, in meters per minute at the surface.

over the northern reefs and makes Enyu Channel an important source of incoming water. It is estimated that the summer average exchange rate is approximately half of the winter rate.

The rate of overturning of the lagoon's primary circulation is estimated to be once in about 150 hours for the winter season and once in approximately 300 hours for the summer season.

The exchange budget for Rongelap Lagoon is based upon less extensive evidence consisting of a week of summer observations during which a steady state can be said to have existed. The measured contribution of each pass and estimated contribution of each reef section is shown in table 5.

The total volume of Rongelap Lagoon is approximately $47 \times 10^9$ cubic meters. Thus 2.2 percent of the lagoon's volume is transported into and out of the lagoon during each tidal cycle. The value is remarkably close to that obtained for Bikini Lagoon. The winter value may be roughly twice as great.

### HORIZONTAL-DIFFUSION RATES

Ten experiments with dye trails and current poles were performed at Bikini to measure the rate of lateral diffusion on the surface. These data are plotted in figure 90 and lines of equal diffusion rate drawn through them, calculated as the rate of expansion in meters per minute of an equivalent dyed spot of water. The values are larger wherever the horizontal component of the secondary circulation of the lagoon is most active. The horizontal expansion of dye spots was observed through the range 50 to 500 meters in diameter and measured in the direction perpendicular

TABLE 5.—*Transport of water per tidal cycle at Rongelap Atoll in the season of doldrums*

[Positive values denote inflow; negative values, outflow]

| Location | Flow, in millions of cubic meters, at— | |
|---|---|---|
| | Flood | Ebb |
| Northeast Pass | 94 | −60 |
| Gogan Pass | 20 | −20 |
| Enybarbar Pass | 200 | −100 |
| South Pass | 630 | −374 |
| Bikien Pass | 44 | −35 |
| Eniran Pass | 35 | −30 |
| Kaeroga Pass | 200 | −200 |
| West Pass | −300 | −300 |
| Total | 923 | −1,110 |
| Northern reefs | 180 | 140 |
| Western reefs | −40 | −65 |
| Total | 140 | 75 |
| Total exchange | 1,063 | −1,054 |

to the local surface current. This is equivalent to a coefficient of horizontal-eddy diffusion of from $0.7 \times 10^4$ square centimeters per second for the lower rates of spread to $1.8 \times 10^4$ square centimeters per second for the higher rates assuming a characteristic radius of 100 meters for the dye spots. These observations apply only in the observed range of dimensions and are probably to be extrapolated in accordance with the "4/3 law" of Richardson (1926). Further data on both the horizontal and vertical diffusion processes have been examined and described by Munk, Ewing, and Revelle (1949).

## LITERATURE CITED

Hess, H. H., 1946, Drowned ancient islands of the Pacific basin: Am. Jour. Sci., v. 244, p. 772–791.

Munk, W. H., and Sargent, Marston C., 1948, Adjustment of Bikini Atoll to ocean waves: Am. Geophys. Union Trans., v. 29, p. 855–860.

Munk, W. H., Ewing, G. C., and Revelle, R. R., 1949, Diffusion in Bikini Lagoon: Am. Geophys. Union Trans., v. 30, p. 59–66.

Nugent, L. E., 1946, Coral reefs in the Gilbert, Marshall, and Caroline Islands: Geol. Soc. America Bull., v. 57, p. 748.

Richardson, L. F., 1926, Atmospheric diffusion shown on a distance-neighbor graph: Royal Soc. of London Proc., (A), v. 110, p. 709, 727.

Sverdrup, H. U., Johnson, M. W., and Fleming, R. H., 1946, The oceans, New York, Prentice Hall Inc.

Tracey, J. I., Jr., Ladd, H. S., and Hoffmeister, J. E., 1948, Reefs of Bikini, Marshall Islands: Geol. Soc. America Bull., v. 59, p. 861–878.

# Adjustment of Bikini Atoll to Ocean Waves

*By* WALTER H. MUNK *and* MARSTON C. SARGENT

Bikini and Nearby Atolls, Marshall Islands

GEOLOGICAL SURVEY PROFESSIONAL PAPER 260-C

UNITED STATES GOVERNMENT PRINTING OFFICE, WASHINGTON : 1954

# CONTENTS



# ILLUSTRATIONS



# TABLES

# ADJUSTMENT OF BIKINI ATOLL TO OCEAN WAVES

By Walter H. Munk and Marston C. Sargent


## ABSTRACT

Atolls in the trade-wind belt withstand a continuous heavy pounding from ocean waves. Against the windward side of Bikini Atoll alone it is estimated that waves dissipate 500,000 horsepower, one-fourth the power generated at Hoover (Boulder) Dam. To withstand these forces, the exposed reefs are molded into a most effective natural breakwater, consisting of long narrow grooves in the seaward face of the reef, and surge channels on the reef flat. These surge channels are tuned to the prevailing wave periods. Their distribution around the reef conforms to the distribution in wave activity, which in turn is controlled by prevailing winds over the north and south equatorial Pacific.

Some of the power of the breaking waves is utilized to maintain a water level just inside the surf zone about 1.5 feet above the general sea level. The water flows downhill over the reef into the lagoon, regardless of the stage of the tide, with an average speed of 0.5 to 1.0 knot, but occasionally with speeds up to 4 knots. The reef as a biological community utilizes this current and maintains thereby a wave-resisting and modifying structure.


## GROOVES AND SURGE CHANNELS

The features to be described here are best developed between Bikini and Aomoen islands (fig. 91), where the reef is directly exposed to the waves of the prevailing trade winds (Tracey, Ladd, and Hoffmeister, 1948). Grooves cut the seaward face of the reef at fairly regular intervals (fig. 92) and give it the appearance of a series of spurs rising from the debris-covered slope of the atoll.

Most of the grooves commence at a depth of 35 to 50 feet, then run up the reef slope into and through the surf zone. At the inner end they may end abruptly or be continued as surge channels, or as tunnels with blowholes under the reef platform. Just inside the

Note.—Contribution from the Scripps Institution of Oceanography, New Series, No. 698.

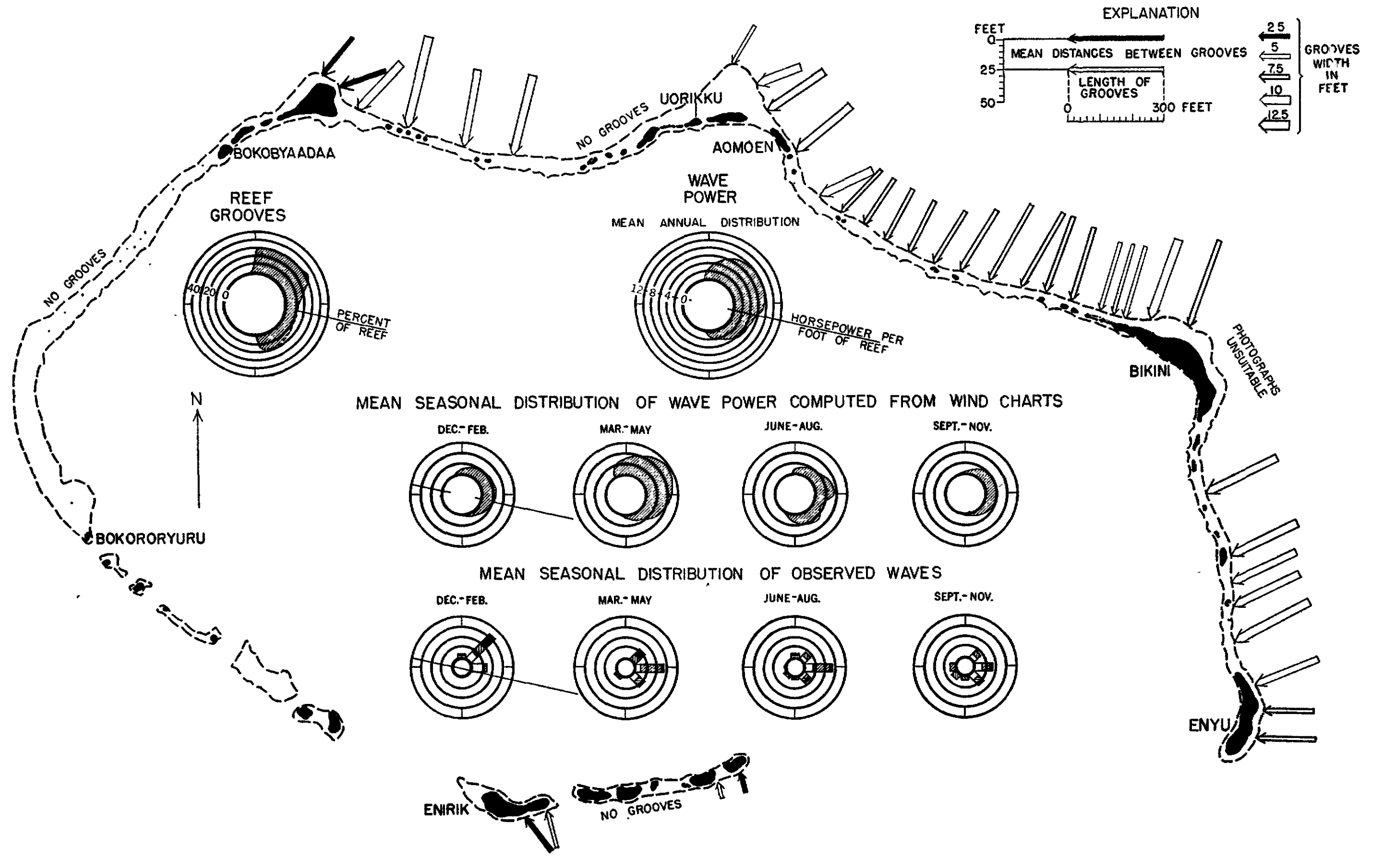


Figure 91.—Distribution of reef grooves and wave power around the reef of Bikini Atoll; the length, width, and spacing of the grooves are proportional to the length, width, and spacing of the arrows drawn against the reef; polar-coordinate graph to the left shows percent of area occupied by grooves as a function of their exposure; polar-coordinate graphs to the right show mean distribution of computed wave power and of observed waves.

surf zone, around the blowholes and the heads of grooves and channels, colonies of *Lithothamnion* and corals rise about 2 feet above the general reef level. The upper faces of the spurs are paved with living *Lithothamnion* which present an extremely rough surface. The sides of the grooves are covered with projecting, often bracketlike colonies. The bottoms of the grooves consist of relatively smooth rock and sand.

Between Bikini and Aomoen islands the grooves are spaced about 25 feet apart, are about 16 feet deep at their inner ends, and vary in width from 3 to 6 feet. The grooves play a vital part in the function of the coral reef as a breakwater. Near their outer ends, which extend to the maximum depth of appreciable wave action (see appendix 1), they interfere with the normal orbital water motion associated with waves on a sloping bottom by "taking the bottom out from under the waves"; at the inner end they pursue a "divide and conquer" policy. The resulting effect on waves is remarkable. To an observer standing on the platform just inside the surf zone, the breakers at first appear to come crashing down upon him; 2 seconds later the wave has virtually disappeared, its momentum converted into a noisy surge which rushes up the channels on each side of the platform. Much of the remaining energy is spent when the surge meets the backrush from the preceding breaker. Wave energy is also dissipated by friction along the sides of the grooves and channels, where an abundant bracketlike growth of organisms is found.

The surge channels are properly tuned to the average wave characteristics (fig. 92). An average depth of 15 to 20 feet and a length of about 200 feet (*li*, in fig. 92) between the outer end of the platform (*Lithothamnion* ridge) and the inner ends of the channels correspond to a fundamental period of oscillation of 8 seconds, which is also the prevailing period of the waves of the trade winds (see appendix 2). As a result, the uprush of each wave will meet the backrush of the preceding wave at approximately midchannel.

### DISTRIBUTION OF GROOVES AND PREVAILING WAVE DIRECTIONS

The dimensions of grooves around the entire reef of Bikini Atoll were estimated from aerial photographs, and are designated by arrows on figure 91. The spacing *s*, width *w*, and outer length *lo* (fig. 92) of the grooves are designated by the spacing, width, and length of the arrows. Photographs of the reef to the south of Bikini island were unsuitable for the determination of the grooves, but it is known that grooves are well developed in that area.

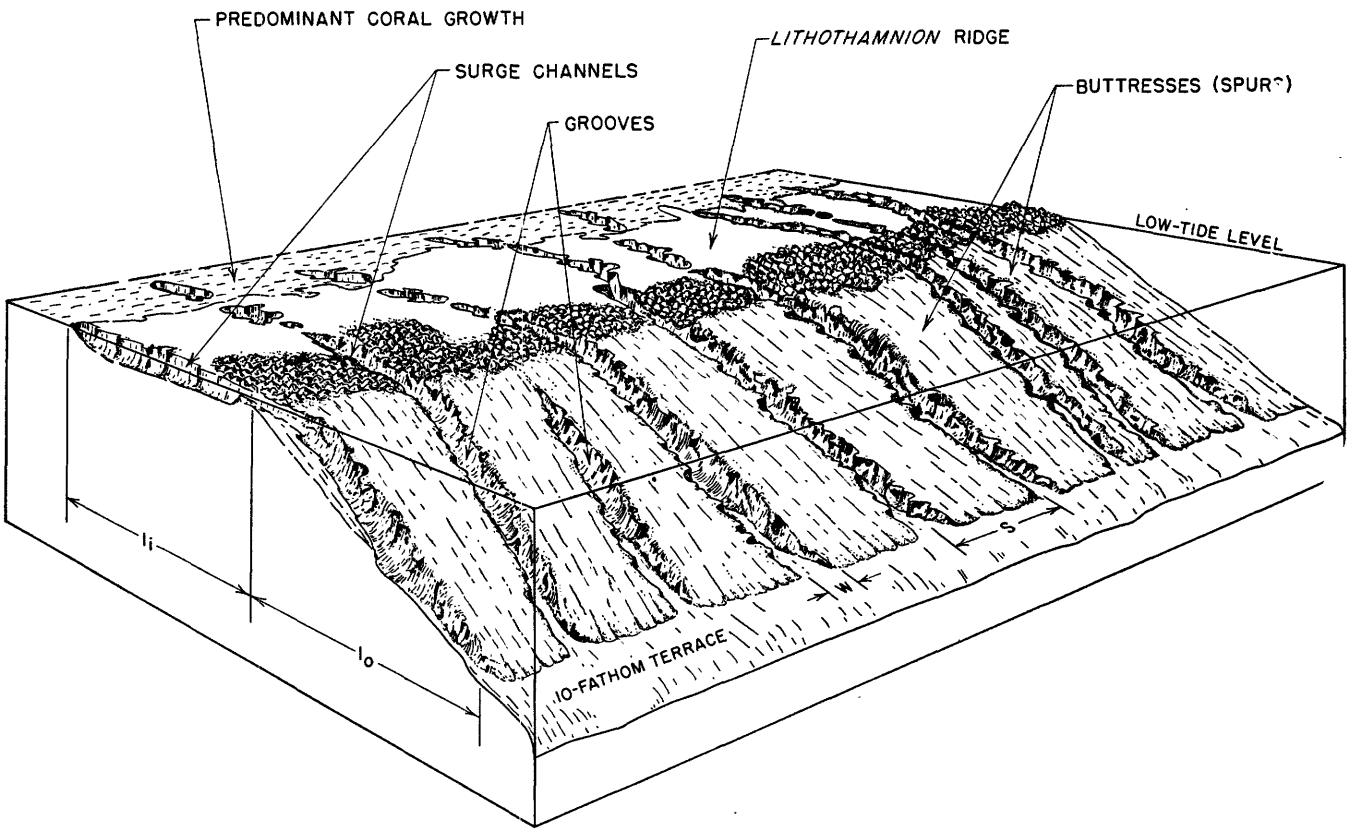


FIGURE 92.—Generalized sketch of seaward face and top of reef on windward side of Bikini Atoll. Original by D. B. Sayner.

The greater length of the grooves with northern exposure relative to those with southern exposure is due to the steeper slope of the reef to the south (Tracey, Ladd, and Hoffmeister, 1948). The absolute depth at which the grooves commence appears to be approximately constant and to extend to the greatest depth for which wave action is appreciable (see appendix 1).

The percent of reef area occupied by the grooves equals $100w/s$. This is plotted as a function of the azimuth of the grooves on the polar coordinate graph on the left in figure 91. No grooves were found where the reef exposure has a westerly component.

The distribution of grooves can be correlated with the distribution of wave power around the atoll. The polar-coordinate graphs to the right in figure 91 give the average seasonal and annual distribution of wave power plotted against reef exposure and expressed in units of horsepower per foot length of reef.

Wave power was computed as follows: The principal generating areas were determined from the "Atlas of climatic charts of the oceans" (U. S. Weather Bureau, 1938); they lie in the trade-wind belts of the north and south Pacific. Swell from the "roaring forties" occasionally reaches the northern Marshall Islands but will be too low to be significant. The frequencies of the prevailing winds in the two main generating areas, and of winds from other directions, were determined from wind roses on the "North and South Pacific pilot charts." The height, period, and direction of waves reaching Bikini Atoll from all directions were then computed, following the method for forecasting sea and swell from weather maps (Sverdrup and Munk, 1946a). Finally the bending of waves around the atoll because of refraction was estimated (Sverdrup and Munk, 1946b) and the wave power computed (see appendix 3).

A rough check of the validity of these computations could be obtained from sea and swell observations appearing in the "Sea and swell charts, northwestern Pacific" (Hydrographic Office 10712C). Averages were formed for each season, taking into account all observations in the area between longitudes 160° and 170° E., and between latitudes 5° and 15° N. These are presented by the wave roses in figure 91. The main features in the observed wave distribution are in agreement with the computed distribution of wave power.

The graph of the annual distribution of wave power is based entirely upon the computed rather than the observed wave characteristics, partly because of the small number of observations but chiefly because the quality of these observations probably is inferior to the quality of the computed values.

The diagrams in figure 91 show a significant correlation between the directional distribution of wave power and reef grooves. Grooves are restricted to reefs with a component of exposure to the east, the direction from which wave action is pronounced. Owing to wave refraction a small portion of the wave power does reach the western sides of the atoll, but there the power dissipated amounts to only a fractional horsepower per foot length of reef, and it appears that at least 1 or 2 horsepower is required for the development of grooves. On the eastern half of the reef the average power delivered by the waves equals 3 horsepower per foot length of reef, or about 20 horsepower per groove.

The distribution of grooves reveals a maximum for an east-northeast exposure, and a secondary maximum for a southeast exposure. These features are associated with the principal wave-generating areas in the tradewind belts of the north Pacific and south Pacific, respectively. The distribution of wave power reveals the same features; except during the summer months the effect of the distant south Pacific trade winds is overshadowed by the effect of the local trade winds. For a corresponding location in southern latitudes the reverse should be true, and the distribution should be a mirror image of the one found at Bikini Atoll.

The bimodal distribution of grooves points toward a wave origin; if the channels were to be attributed to direct wind action, the development in the southeast quarter would be missing.

## ECOLOGICAL SIGNIFICANCE OF WAVE ACTION

The mechanisms by which wave action governs the growth and distribution of reef-building organisms in such a way as to mold the reef cannot be clarified in any detail by data in our possession. It is clear in general that the reef form represents some kind of equilibrium between the erosive or destructive power of the waves and the growth potential of the reef-building organisms. It is generally apparent that in areas where the wave action and hence presumably destructive power is greatest, growth of reef builders is also most rapid (Yonge, 1940, p. 355, 374). Hence windward reef faces may be nearly in equilibrium under conditions of rapid growth and erosion, leeward ones under slow growth and erosion.

The mechanism by which waves promote growth has not usually been distinguished from that of currents. Water motion induced by the waves has been considered to supply nutrients in a broad sense, including gases, mineral nutrients, and sometimes particulate organic matter to the reef organisms. Its importance in removing excreta should also be recognized. That these items can be supplied, or removed, as well by currents as by waves has not usually been mentioned, probably because most previous work has been done on fringing and barrier reefs where transreef currents are small. At Bikini Atoll the current across both windward and leeward reefs is of the order of one knot (30 to 80 centimeters per second), and the mass transport of water through a vertical square centimeter is about a liter every 20 seconds. In the presence of such an abundant supply of nutrient-bearing water (in the widest sense), some other explanation must be sought for the paramount importance of wave action.

In view of the fact that colonies of *Lithothamnion* grow mainly on the wave-beaten edge of the reefs although the waters over the whole reef show no impoverishment of nutrients, it is suggested that the scrubbing action of violently breaking waves is critical. Such action might prevent the settling of particulate matter and the establishment of sessile organisms which could interfere with the nutrient supply and the waste excretion of the reef builders. The erosive action of high-velocity currents has been estimated by Hjulstrom (see appendix 1). It is also possible that the rapid turbulent motion in breaking waves is effective because it rapidly renews the film of water in immediate contact with the surface of the reef-building organisms. Under these conditions molecular diffusion to and from the organism would be entirely eliminated as a possible bottleneck. This suggestion is in accordance with the fact that in the cultivation of small organisms various degrees of stirring are often important. In surf the momentary high velocities in all directions may be effective in stimulating the growth of reef builders—and of the attached surf zone organisms of other localities—even though the net velocity or transport of water and its contents across the reef over a long period of time is practically zero.

The reasons for the changes in frequency and width of grooves and spurs with azimuth are not clear to us. The existence of grooves and spurs strongly suggests a cellular circulation in the water, whether caused and maintained by factors independent of the existence of grooves or spurs or maintained by these features however originated. Tracey, Ladd, and Hoffmeister (1948, p. 873) reasonably propose that the grooves are kept open by a riverlike flow of debris from the reef above and from adjacent spurs and point to the fact that on any vertical plane parallel to the surf zone the orbital velocity of water motion is higher on the spurs than in the grooves. This is a kind of cellular circulation, but it does not for us throw light on the relation between azimuth and groove frequency and width evident in figure 91.

## HEAD OF WATER AT REEF EDGE

Not all the energy of the incoming waves is dissipated by friction. Some energy is converted into potential energy to maintain a water level at the outer edge of the reef at about two feet above the mean water level of the ocean and lagoon water. If the entire wave energy were to be consumed in lifting the water which flows over the reef, the level of this volume of water could be maintained 42 feet above the mean sea level (see appendix 3). Therefore only about 5 percent of the wave's energy is utilized to raise the water level, and 95 percent is dissipated by friction, a large part of it within the surge channels.

In designing artificial breakwaters it may be worth while to consider the lines of a coral reef. These natural breakwaters over a period of thousands of years have evolved into structures admirably suited to withstand the wave forces. Artificial surge channels have in fact been employed on the south coast of the Mediterranean in the generation of electricity by means of wave power. These channels were relatively wide at their outer end and converged gradually toward the inner end. In this manner the water level in a reservoir was maintained at an average elevation of 40 feet above the mean sea level.

## WAVE-DRIVEN CURRENTS OVER THE REEF

From the region of maximum elevation the current flows into the lagoon under the influence of gravity assisted by wind traction. Between Bikini and Aomoen islands, the speed is about 1 foot per second, except during spring low tides, when the retarding effect of bottom friction is disproportionally large, this speed is remarkably independent of tide. In the presence of obstructions the wave-driven current may give rise to striking features. For example, a few days after the arrival of the U. S. S. *Bowditch* a 100-foot channel broke through the sandspit at the northwest end of Bikini island, and water flowed through this channel in a steady stream for almost 6 months.

Currents over the reef were measured by dropping dye bombs from planes and taking timed photographs of the drifting color patches (Von Arx, 1948). Between February and April 1946, while the trade winds blew predominantly from the east-northeast, wave-driven currents flowed into the lagoon over the entire eastern and northern reefs, adding $3 \times 10^{14}$ cubic centimeters of water, 1 percent of the entire lagoon volume, during each 12-hour interval. During an equal time interval the tidal flow—chiefly through the deep southwesterly passages—amounted to 2 percent of the lagoon volume. Although the oscillating tidal current represented the principal component of water exchange between the ocean and the lagoon, the one-directional wave-driven current is of primary importance to the renewal of water in the lagoon. This renewal was of interest with regard to the flushing of radio-active water out of the lagoon.

The wave-driven current is important also for another reason. At noon, especially during low tide, the water over the reef becomes warmer, more saline, and supersaturated with oxygen. Upon entering the lagoon, this "reef water" may be recognized as a distinct water type. The mixing of this water with the lagoon water provided a method for computing the rate of vertical diffusion (Munk, Ewing, and Revelle, 1949).

## DISCUSSION AND CONCLUSIONS

Waves breaking over coral reefs may lead to the formation of grooves and the flow of currents over the reef. The only other known examples of currents due to wave action are longshore currents and rip currents caused by waves breaking on gently sloping beaches (Munk and Traylor, 1947). Since the waves represent an integrated effect of the winds, their energy being accumulated during many hours, and over thousands of miles, a wave-driven current assures a steadier supply of water than a current maintained by local winds.

The waves and the wave-driven current may be of biological significance in three ways. First, they permit luxuriant growth of *Lithothamnion* and other encrusting coralline algae in situations exposed to the heaviest wave action. Second, the current maintains a nearly constant supply of mineral nutrients and dissolved gases over the whole width of the reef (Sargent and Austin, 1949). Third, as noted above, the current, which at noon is supersaturated with oxygen, carries water into the lagoon.

## ACKNOWLEDGMENT

This work represents results of research carried out for the Hydrographic Office, the Office of Naval Research, and the Bureau of Ships of the Navy Department under contract with the University of California. The original of figure 92 was drawn by D. B. Sayner.

## APPENDIX 1.—DEPTH OF WAVE ACTION

The average speed of water movement along the bottom in water of depth $h$ is given by

$$u=2\pi \frac{H}{T} \sinh^{-1}\left(\frac{2\pi h}{L}\right) \qquad (1)$$

where $H$ and $T$ are the height and period of the wave responsible for the water movement. The wave length is given by

$$L=\frac{gT^2}{2\pi} \tanh\left(\frac{2\pi h}{L}\right) \qquad (2)$$

where $g$ is the acceleration due to gravity. For a wind speed of 16 knots, blowing over a long fetch and for a long time, the wave height and period equal 7 feet and 8 seconds, respectively (Sverdrup and Munk, 1946a). These figures are in agreement with the observed dimensions of trade-wind waves. Simultaneous solution of (1) and (2) leads to the numerical values shown in table 1. The outer ends of the grooves fall into a depth of about 50 feet, where the average speed due to wave action is about 1.2 feet per second. The third column shows the size of particles which can be eroded by a current of speed $u$, based upon measurements in rivers by Hjulstrom (Trask, 1939, pp. 10–11). According to Hjulstrom, ". . . fine sand, which has a diameter of 0.3 to 0.6 mm, is the easiest to erode, whereas both silt and clay on the one hand and coarse sand and gravel on the other require higher velocities." If these conclusions are applicable here, they indicate that no erosion can take place for current speeds less than 0.5 feet per second—that is, at depths exceeding 100 feet, no matter how small the size of the grains.

TABLE 1.—*Mean orbital speed on the ocean bottom*

| Depth $h$ (feet) | Speed $u$ (ft/sec) | Size of particles which can be eroded (mm) |
|---|---|---|
| 50 | 1.2 | 3 |
| 75 | .8 | 1 |
| 100 | .5 | .05 |
| 125 | .3 | (1) |

1 No erosion.

At a depth of 50 to 75 feet the reef slope is relatively gentle, forming virtually a terrace (Tracey, Ladd, and Hoffmeister, 1948). One would be tempted to ascribe this "10-fathom terrace" to wave action were it not for the fact that it is also found inside the lagoon.

## APPENDIX 2.—DIMENSIONS OF SURGE CHANNELS

The speed of a surge in a channel equals approximately $\sqrt{gh}$, where $h$ is the depth of the water measured from the highest point in the surge. For effective interference the surge must travel a distance of roughly the length of the channel during one wave period (fig. 93). The corresponding length of the channel equals approximately $T\sqrt{gh}$. Setting $g=32.2$ feet per second and $h=15$ feet, leads to the values shown in table 2.

TABLE 2.—*Length of channels for maximum interference*

| Period T (seconds) | Length (feet) |
|---|---|
| 6 | 130 |
| 8 | 175 |
| 10 | 220 |

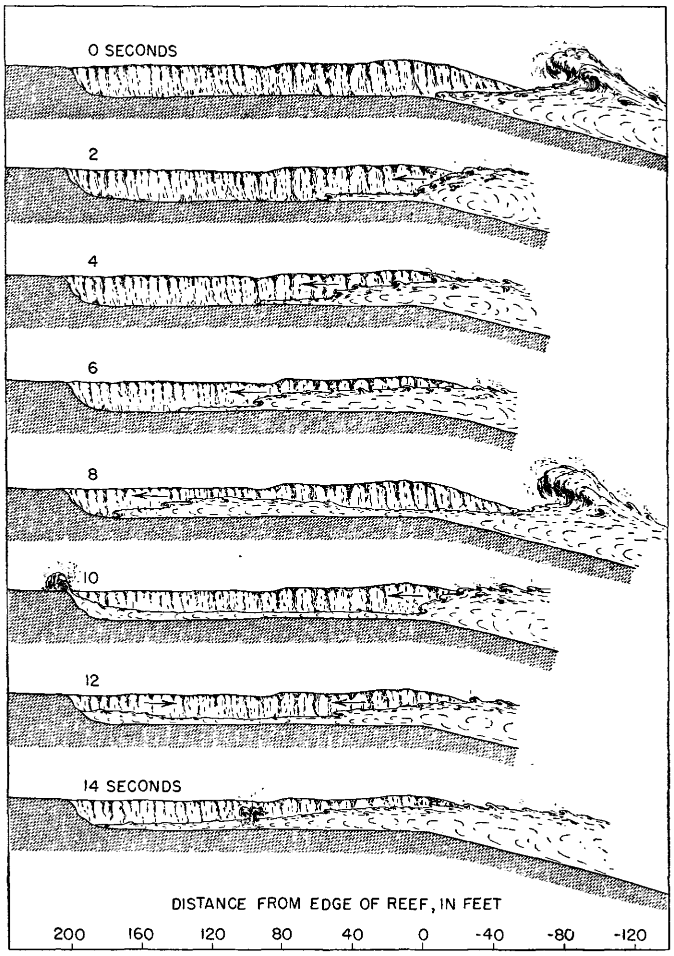


FIGURE 93.—Breaking wave produces surge which travels up the surge channels, is reflected on the upper end, and meets surge from subsequent breaker midchannel; surge channels are tuned to the period of prevailing waves.

The wave period in the region of the northern Marshalls is remarkably constant and falls within the limits of 7 to 9 seconds, probably more than 90 percent of the time. Over most ocean areas the period of the significant waves varies between such wide limits (probably 6 to 14 seconds) that resonance for any permanent structure would be achieved only a small fraction of the time.

## APPENDIX 3.—WAVE POWER

The mean energy dissipated by the waves each second against a unit width of reef is $(1/32\pi)\rho g^2H^2T$ where $\rho$ is the density of water. The transport of water per foot width of reef equals $h'V$ where $h'$ is the depth of water over the reef, $V$ the corresponding speed of flow. If the entire wave energy were to be utilized in raising the water flowing over the reef, then

$$\frac{1}{32\pi}\rho g^2H^2T=\rho g h' V s, \qquad (3)$$

so that the vertical distance through which the water would be raised is

$$s=\frac{g}{32\pi}\frac{H^2T}{h'V}.$$

Setting $H=7$ feet, $T=8$ seconds, $h'=3$ feet, and $V=1$ foot/second gives $s=42$ feet.

## LITERATURE CITED

Munk, W. H., and Traylor, M. A., 1947, Refraction of ocean wave, a process linking underwater topography to beach erosion: Jour. Geol., v. 55, p. 1–26.

Munk, W. H., Ewing, G. C., and Revelle, R. R., 1949, Diffusion in Bikini Lagoon: Am. Geophys. Union Trans., v. 30, p. 59–66.

Sargent, M. C., and Austin, T. S., 1949, Organic productivity of an atoll: Am. Geophys. Union Trans., v. 30, p. 245–249.

Sverdrup, H. U., and Munk, W. H., 1946a, Empirical and theoretical relations between wind, sea, and swell: Am. Geophys. Union Trans., v. 27, p. 823–827.

——— 1946b, Theoretical and empirical relations in forecasting breakers and surf: Am. Geophys. Union Trans., v. 27, p. 828–836.

Tracey, J. I., Jr., Ladd, H. S., and Hoffmeister, J. E., 1948, Reefs of Bikini, Marshall Islands: Geol. Soc. America Bull., v. 59, p. 861–878.

Trask, P. D. (Ed.), 1939, Recent marine sediments: Am. Assoc. Petroleum Geologists Bull., Tulsa, 736 p.

United States Weather Bureau, 1938, Atlas of climatic charts of the oceans, U. S. Govt. Printing Office.

Von Arx, W. S., 1948, The circulation of Bikini and Rongelap Lagoons: Am. Geophys. Union Trans., v. 29, p. 861–870.

Yonge, C. M., 1940, The biology of reef-building corals: Sci. Repts. Great Barrier Reef Exp., v. 1, p. 353–389.

# Sea Temperature in the Marshall Islands Area

*By* MARGARET K. ROBINSON

Bikini and Nearby Atolls, Marshall Islands

GEOLOGICAL SURVEY PROFESSIONAL PAPER 260-D

UNITED STATES GOVERNMENT PRINTING OFFICE, WASHINGTON : 1954

# CONTENTS



# ILLUSTRATIONS

[Plates 74-79, in pocket]



# TABLES

# BIKINI AND NEARBY ATOLLS, MARSHALL ISLANDS

## SEA TEMPERATURE IN THE MARSHALL ISLANDS AREA

By Margaret K. Robinson


### ABSTRACT

Horizontal distribution of average sea temperature, based on 6,766 bathythermograms in the Marshall Islands area, 20° N.–5° S., 155° E.–175° W. is presented in charts of average temperature for each month, for the surface and for the 200-, 300-, and 400-foot levels, together with charts of maximum, minimum and range of average monthly temperatures and the annual average for the same depths. Analysis of the temperature distribution shown on these charts indicates that there are two major seasonal regimes: a summer regime from April to August, characterized at 400 feet by large-scale cold cells on both sides of the Marshall and Gilbert Islands chain; a winter regime from October to February, characterized at the same depth by a tongue of cold water, at about 8° N., which runs directly across the area. Certain conclusions concerning the currents can be drawn from the pattern of isotherms shown on the horizontal charts. The Marshall and Gilbert Islands chain appears to be a topographical barrier across the Equatorial Current system giving rise to large-scale eddies in the North Equatorial Current, the Equatorial Countercurrent, and possibly the South Equatorial Current. There are evidently seasonal changes in the position of the currents and in the formation of the eddies. There appears to be an eastward flow north and west of the Marshall Islands.

Smoothed average-annual-temperature curves for each 5-degree square in the area are presented for the surface and for depths of 100, 200, 300, 350, and 400 feet. The annual curves show seasonal cycles not immediately apparent in the horizontal charts. North of 10° N. there is a single annual cycle for the surface and the 100- and 200-foot curves. South of 10° N. a double temperature cycle develops in the same levels. This double cycle is also seen in some 5-degree squares south of the equator. The curves for the lower levels, which are associated with the depth of the thermocline, frequently show inverse relationships with the surface curves.

Fourteen vertical sections of temperature across the Equatorial Currents, based on individual bathythermograph observations, between Longitudes 163° E. and 120° W., are given. These sections show that there are marked differences in the width of the Equatorial Countercurrent and in the depth of the thermocline in the current boundary zones, going from east to west across the Pacific Ocean; and that temperatures inimical to coral reef growth in the Eastern Pacific are found in the euphotic zone.

Charts of temperature distribution at two different times in the 1-degree square surrounding Bikini Atoll for the surface, and for the 200-, 300-, 400-, 600-, and 800-foot levels are shown. These charts illustrate possible deviations from the average values of the monthly charts which might be expected within a 1-degree square.


Note.—Contribution from The Scripps Institution of Oceanography, New Series No. 700.

### INTRODUCTION

In order to provide an average environmental background of ocean temperature for the scientific research in biology and geology done at Bikini Atoll and in the Marshall Islands, this analysis of 6,766 bathythermograms for the area latitude 20° N. to 5° S., longitude 155° E. to 175° W. has been made. The average-temperature distributions based on this analysis can also be used to make qualitative inferences about the ocean currents in the area.

Temperature and salinity data obtained from Nansen bottles and reversing thermometers in the Marshall Islands are insufficient for a detailed picture—of such importance to the biologist—of the surface layers of the sea at depths of less than 400 feet. On the other hand, the accuracy of reversing thermometers cannot be claimed for bathythermograph readings. In the oceanic area between Hawaii and California average temperatures based on these readings were shown to have a positive bias of 1.0° F in comparison with temperatures measured with reversing thermometers.[1] The amount of bias in the readings for this area has not been accurately ascertained, but visual comparison of the temperature distribution in this study with that based on reversing thermometer measurements (Barnes, Bumpus, and Lyman, 1948, and Mao and Yoshida, 1954) will show the temperatures of this study also to be warmer on the average by approximately 1.0° F. However, average temperatures based on bathythermograms give excellent relative pictures of temperature distribution at constant level or in vertical sections, and absolute temperature values can be inferred from comparisons with accurate reversing-thermometer data.

The author wishes to express thanks and appreciation to Dr. Roger Revelle for his personal assistance and beneficial criticisms during the preparation of this temperature study.

### DISTRIBUTION OF BATHYTHERMOGRAMS

This study is based on 6,766 individual bathythermograph readings taken by U. S. Navy and U. S. Coast

[1] Robinson, M. K., 1951, Sea Temperature in the North Pacific Area, lat. 20°–40°. N., long. 125°–155° W.: Scripps Inst. Oceanography, Reference 51-20, September 15, 1951.

Guard ships between 1942 and 1951. These bathythermograms—the photographic reproductions of the original glass slide used in the bathythermographs—are on file at the Scripps Institution of Oceanography. Figure 94 gives the total space distribution of the observations; figures 95 and 96 give the space distribution by months. In table 1 the time distribution of the data in percentages by years has been tabulated; in table 2 the time distribution is given in percentages by months.

TABLE 1.—*Time distribution of bathythermograms, by years*

| Year | Percent | Year | Percent | Year | Percent |
|---|---|---|---|---|---|
| 1942 | 0.3 | 1946 | 7 | 1949 | 0 |
| 1943 | 1.7 | 1947 | 3 | 1950 | 2 |
| 1944 | 49 | 1948 | 3 | 1951 | 2 |
| 1945 | 32 | | | | |

TABLE 2.—*Time distribution of bathythermograms, by months*

| Month | Percent | Month | Percent | Month | Percent |
|---|---|---|---|---|---|
| January | 4 | May | 5 | September | 9 |
| February | 8 | June | 11 | October | 6 |
| March | 12 | July | 10 | November | 21 |
| April | 8 | August | 12 | December | 6 |

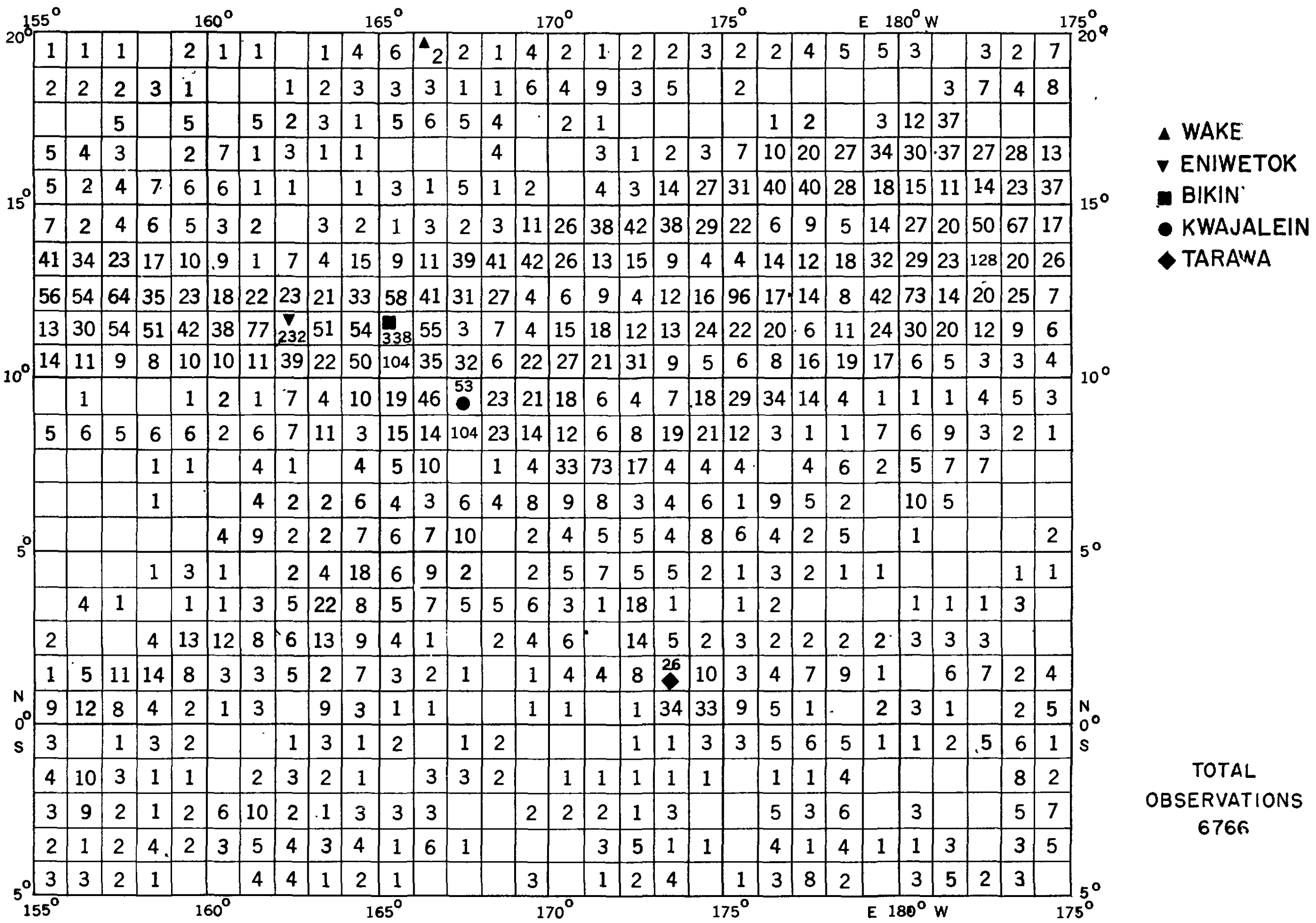


FIGURE 94.—Distribution of bathythermograph observations—total.

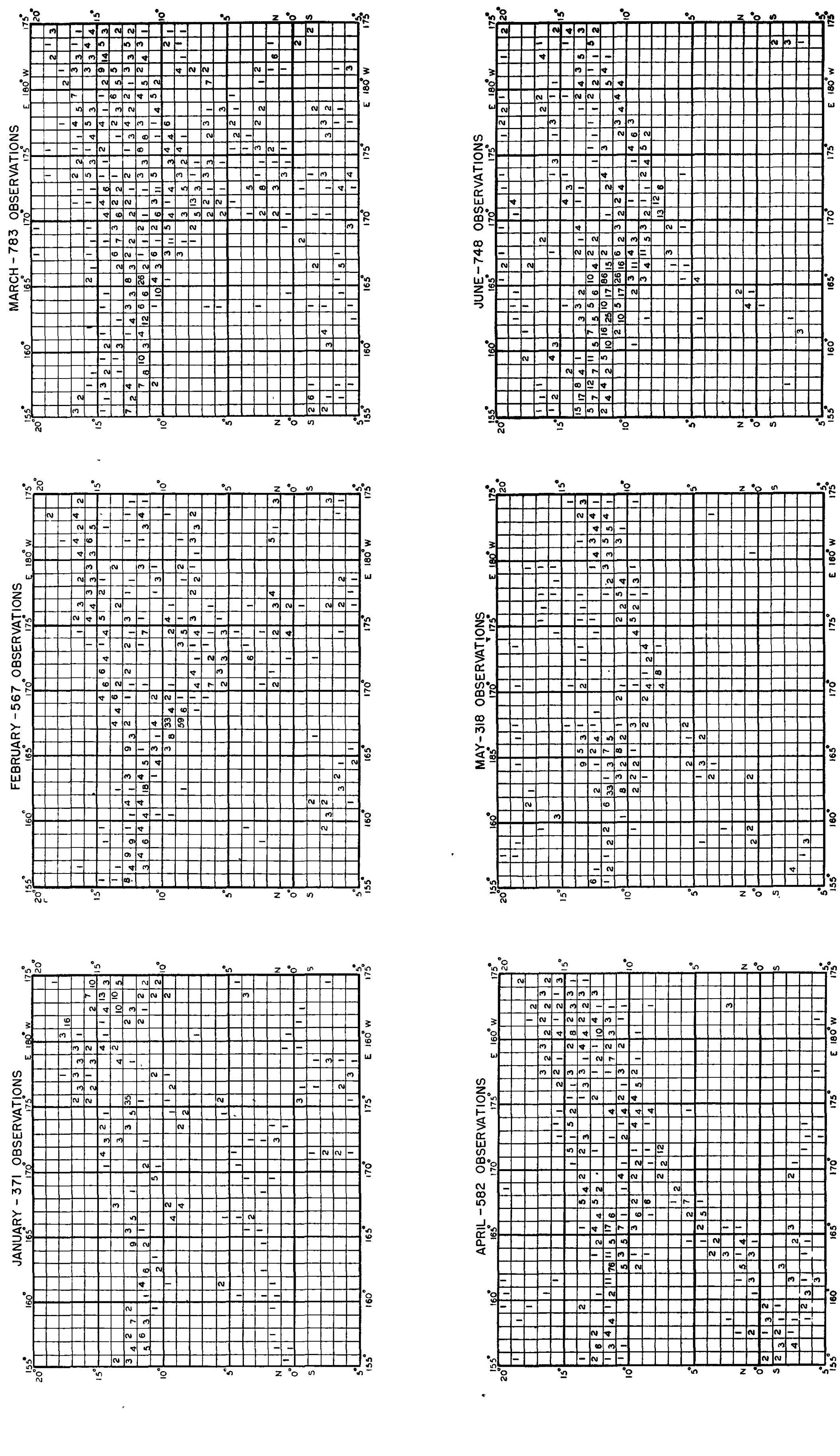


FIGURE 95.—Distribution of bathythermograph observations—January–June.

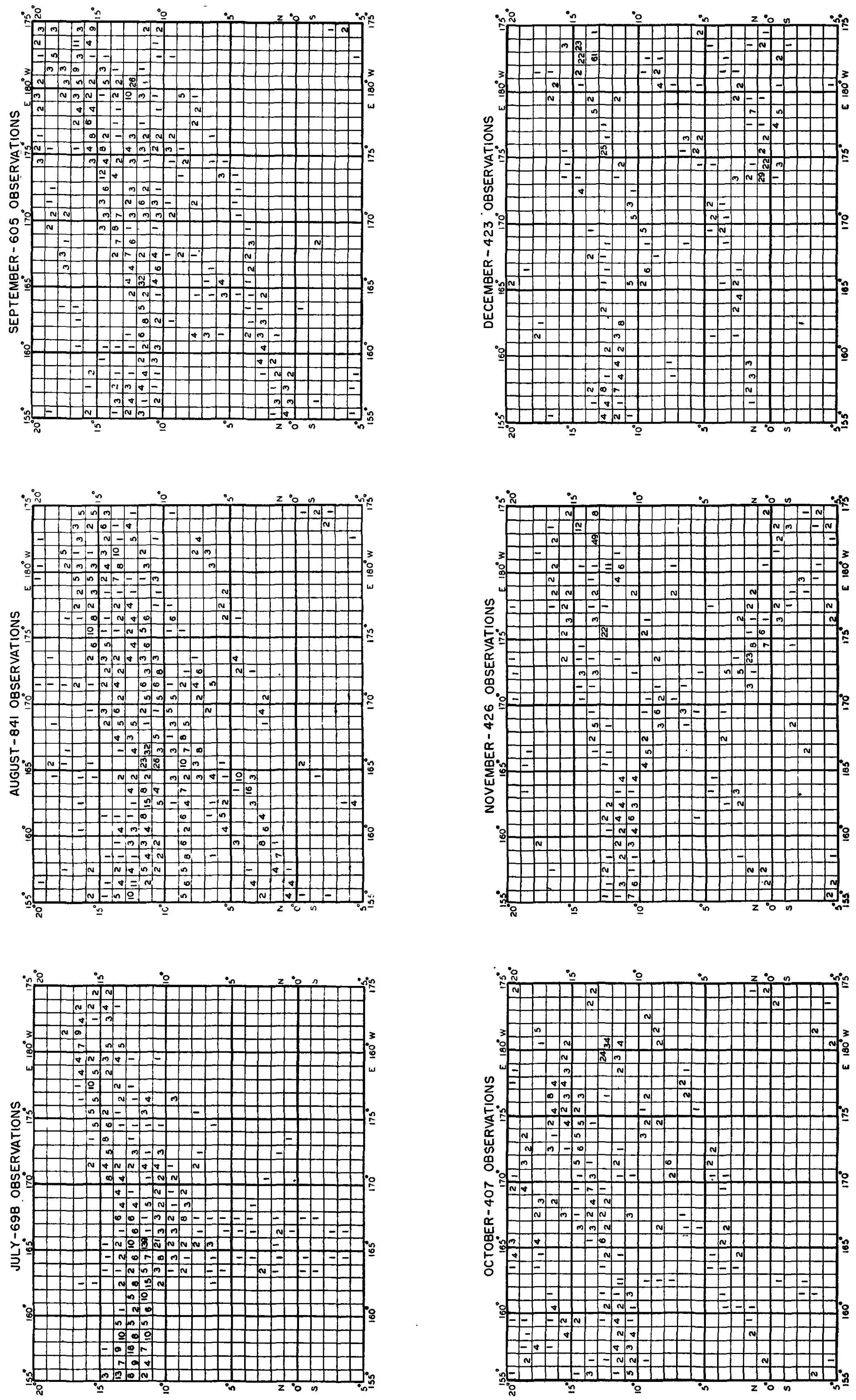


FIGURE 96.—Distribution of bathythermograph observations—July–December.

## METHOD OF ANALYZING DATA

Temperatures at the surface and at depths of 100, 200, 300, 350, and 400 feet were read from all bathythermograms, averaged arithmetically by months and by 1-degree squares and entered on base maps of the area. Next, all values for each level within each 5-degree square (twenty-five 1-degree squares) were averaged by months and plotted against time. Smooth annual curves for each level and for each 5-degree square were drawn (fig. 97). In several squares, where no data are available for certain months, this required considerable interpolation. The annual curves were checked for consistency by comparing them from level to level and by drawing for each month an average temperature-depth curve from the annual curve values of each 5-degree square. Values for each 5-degree square for each month and depth were then read from the annual curves and entered on transparent sheets, which were used as overlay sheets for charts on which the average values for 1-degree squares had been entered. The first drawing of the isotherms was made on these overlay sheets. Contours were based on the average values for 1-degree squares where available; where these are lacking, the average values for 5-degree squares from the annual curves were used. In the final draft, minor irregularities based on values for 1-degree squares were smoothed out when they appeared to be inconsistent with the over-all picture.

Plates 74, 75, and 76 present the horizontal temperature distribution by months. Dashed lines (based on 5-degree squares) have been used to indicate where the isotherms are based on values from the annual curves shown in figure 97. Solid lines indicate values based on one-degree squares. The 100-foot and 350-foot charts were eliminated from the final results; values for these levels, however, are included in the annual curves (fig. 97).

Plate 77 comprises four charts showing average temperatures: the maximum average; the minimum average; the range of the average; and the annual average. These four charts are based on the averages for 5-degree squares.

## HORIZONTAL DISTRIBUTION OF TEMPERATURE

There are several prominent features in the horizontal distribution charts which reflect the presence of the North and South Equatorial Currents and the Equatorial Countercurrent, as well as the effect of the topographic barrier across the current systems presented by the Marshall and the Gilbert Islands.

Two major seasonal regimes are evident in the horizontal distribution charts: a summer regime from April to August, a winter regime from October to February. March and September are transition months.

These seasonal differences can best be seen by comparing the 400-foot charts of the different months. At this depth the winter regime is characterized by a tongue of cold water, its axis usually at about 8° N., which runs directly across the area from December to March, but which has a saddle point near the Marshall Islands from September to November. During these months the tongue has a slight southwest trend east of the Marshall Islands. From September to December there is a warm tongue whose axis points northeast through the gap between the Marshall and the Gilbert Islands from south of the equator at 155° E. longitude. In the vicinity of the Gilbert Islands, from September to December, the isotherms bend around to form a cold tongue near the equator. North and west of the Marshall Islands, from September to February, there is a warm tongue near 15° N. whose trend is approximately eastward. North of this tongue there is a considerable decrease in temperature in the vicinity of Wake Island.

Beginning with April we see a greatly different pattern at the 400-foot depth level. There is a wedge of warm water west of the Gilbert Islands extending north of the Marshall Islands which divides the southern part of the area into two large cold cells. In some months the colder water appears within the western cell, in others within the eastern cell. During these months, as in winter, we find a warm tongue north and west of the Marshall Islands, with decreasing temperatures near Wake Island.

The surface charts differ markedly in appearance from the 400-foot charts, chiefly because the range of temperature at the surface is much smaller than at 400 feet. But there are also important differences in the pattern of the isotherms.

At the surface from September through March we find a warm tongue from the southwest whose axis extends directly through the island gap and also a tongue of cooler water from the northeast whose axis generally parallels that of the warm tongue. But while the effects of the warm tongue usually are evident beyond the gap between the Marshall and the Gilbert Islands, the cool tongue tends to be blocked by the Marshall Islands. Inspection will show that these surface features are displaced relative to their counterparts at 400 feet. During the northern winter there is also a cool tongue in the southeast whose axis shifts north and south of the equator, but whose approach is usually directly from the east. At times the axis is directed through the Gilbert Islands, at other times it is deflected to the north or south, and in the month of January the tongue terminates east of the Gilbert Islands. This tongue is better defined in the surface charts than in the 400-foot charts. It is interesting to note that in December the coldest water in the entire area at the surface is at the equator at 175° W. longitude. This cool water appears to be associated with divergence in the South Equatorial Current. Contrary to expectations, it is not evident across the entire area. The warm tongue north and west of the Marshall Islands shown on the 400-foot charts is also evident at the surface during the winter months, but it is more variable in position and trend than at 400 feet.

This warm tongue is also present at the surface during certain summer months. The main difference between the summer and winter regimes at the surface is that in summer the warm tongue from the southwest is poorly defined and variable. This warm tongue, which also can be seen in the lower-level charts, is thought to be associated with convergence between the Equatorial Countercurrent and the South Equatorial Current, and the cool tongue from the northeast is thought to be associated with divergence between the Equatorial Countercurrent and North Equatorial Current.

The 200-foot charts are very similar to the surface charts because the thermocline is generally below this level throughout the area. However at 300 feet marked changes begin to occur due to differences in thermocline depth within the area, the full effect of which is seen on the 400-foot charts described above.

Certain conclusions concerning the currents can be drawn from the pattern of isotherms shown on the horizontal charts. The Marshall and the Gilbert Islands chain appears to be a topographical barrier across the Equatorial Current system giving rise to large-scale eddies in the North Equatorial Current and the Equatorial Countercurrent. There are evidently seasonal changes in the position of the currents and in the formation of eddies. During some months the Equatorial Countercurrent appears to flow directly through the gap between the islands. The diagonal trend of the isotherms associated with the Equatorial Countercurrent confirms the opinion of Sverdrup, Johnson, and Fleming (1942), and Mao and Yoshida (1954) that the Equatorial Countercurrent may be found on both sides of the equator. During some months the South Equatorial Current appears to flow to the north of the Gilbert Islands, in other months to the south of them. The tongue of cool water at the equator associated with this current goes beyond the islands in some months, but appears to be stopped by them in others, indicating an eddy also in the South Equatorial Current. The warm water north and west of the Marshall Islands appears to be associated with an eastward flow found by Barnes, Bumpus, and Lyman (1948), and Mao and Yoshida (1954).

The charts on plate 77 show, respectively, the maximum, the minimum, and the range of average monthly temperatures and the annual average. Along the island chains the average range of temperature at and above 300 feet is only about 3° F. Because of the shifting depth of the thermocline, the range at 400 feet is much greater, rising to 10° F. in the southern Marshall Islands.

### SMOOTHED AVERAGE-ANNUAL-TEMPERATURE CURVES

In figure 97 are presented smoothed average-annual-temperature curves for each of the thirty 5-degree squares in the area. As shown in figures 95 and 96 the numbers of observations on which these curves are based differ widely. For example, the curves for the three 5-degree squares between 10°–15° N., 155°–160° E., 160°–165° E. and 165°–170° E. contain practically no interpolations or smoothing, while the lower levels of the three 5-degree squares from 0°–5° S., east of 170° E. are based upon very few observations and should be considered as a first approximation only. Where a large number of observations were available, year-to-year variation and individual erratic values would be eliminated from the curves.

Annual-temperature curves show seasonal cycles not immediately apparent in the horizontal charts. North of 10° N., these curves show a single annual cycle for the surface, and at 100 and 200 feet, with minimum temperatures in February and March and maximum temperatures in September and October. However, in several squares the temperatures do not increase continuously from March to October but remain nearly constant in June, July and August.

Between 5° and 10° N., the leveling off in June and July in the upper levels above the thermocline becomes a double cycle with secondary maxima and minima. Just as there is a lag in the maximum temperature in the north from the time the sun is at its most northerly position, there are also marked differences in phase at these latitudes between the sun's passage and the times of maximum and minimum temperatures. A double cycle is also found in some squares south of the equator. The two 5-degree squares, 0°–5° N., 155°–160° E., and 0°–5° S., 155°–160° E., show an anomalous one-cycle curve above the thermocline with minimum temperatures in June and maximum temperatures in October. The annual range of temperature at the surface is only 2.8° F, and here the highest temperatures of the entire area are found throughout the year. In this area of minimum annual range of temperature the effects of the shifting position of the Equatorial Countercurrent completely overshadow the effects of the sun's passage.

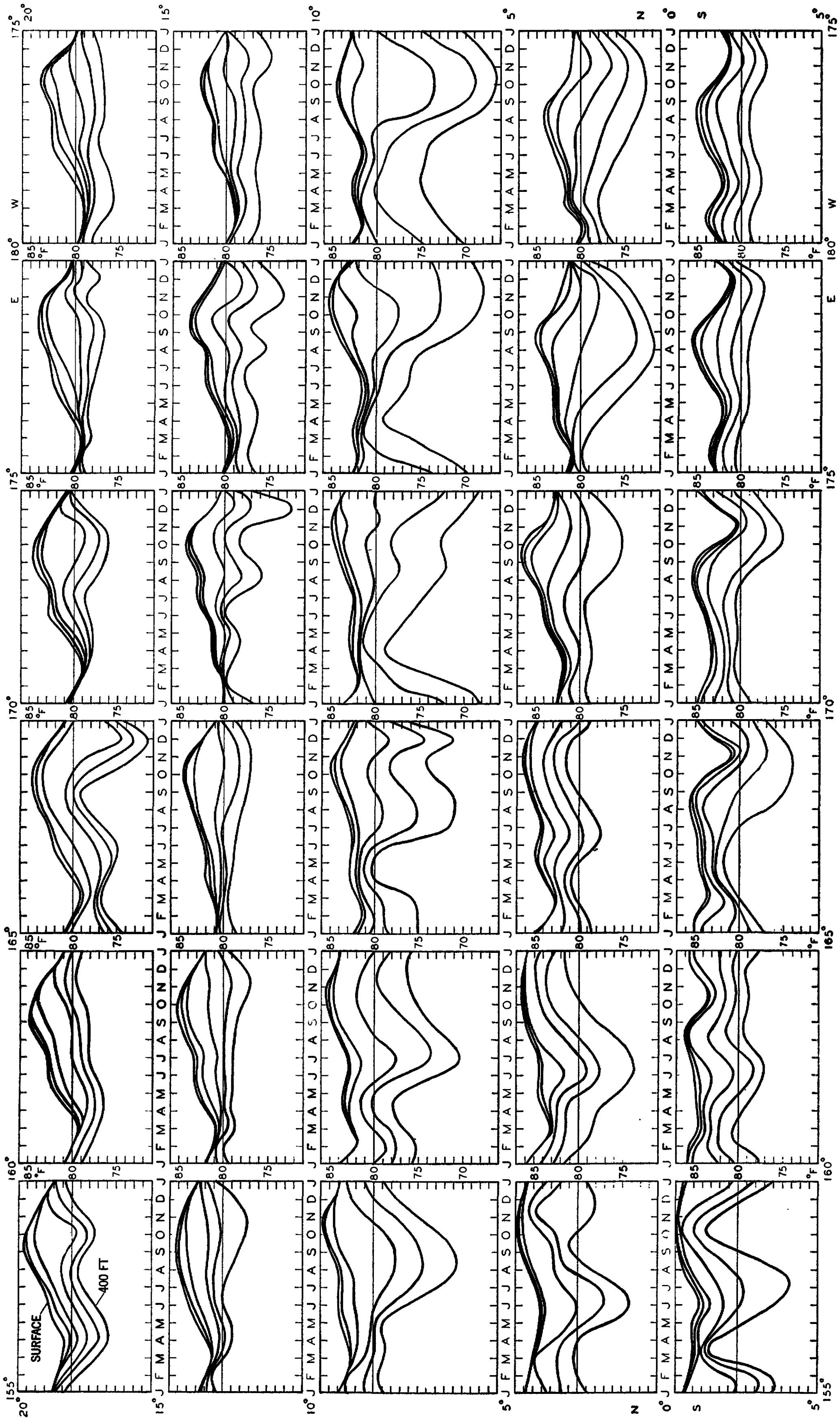


FIGURE 97.—Annual-temperature curves for 5-degree squares at the surface and at depths of 100, 200, 300, 350, and 400 feet.

Temperatures at 300, 350, and 400 feet are related primarily to the depth of the thermocline and the curves for these depths frequently show inverse relationships with the surface curves. The 5-degree square, 15°–20° N., 170°–175° E., is an example. In this square the thermocline is below 400 feet in February and March and near 200 feet late in summer.

The curves of the lower levels between 5° and 10° N. and, to some extent, from 0° to 5° N. show the dramatic results of the shallow thermoclines in the transition zone between the North Equatorial Current and the Equatorial Countercurrent. It is regrettable that the data upon which these curves were based were not so complete as those north of 10° N. It is thus not possible to say to what extent these curves represent the average or typical position of the currents or how much they may be biased by the distribution of the data, the year-to-year variation, internal waves, and observational errors.

From 0°–5° S. very few data were obtained in the lower levels east of the Gilbert Islands, and these curves, which tend to parallel the surface curves, may not be valid; however, in the horizontal charts, the temperature distribution based on these values appears to be consistent with the surrounding values. The three 5-degree squares west of the Gilbert Islands were based on more data but are quite different one from another. If the shapes of these curves, which are represented as a first approximation, are found to be typical on the basis of additional data, their differences can be explained only as results of the shifting currents.

### VERTICAL SECTIONS OF TEMPERATURE ACROSS THE EQUATORIAL CURRENTS

Fourteen vertical sections of temperature, based on individual bathythermograms, have been selected to show differences with longitude. All sections are presented on the same latitude and depth scale. Plate 78 shows vertical-temperature sections based on observations taken aboard the U. S. S. *Barton*, U. S. S. *O'Brien*, U. S. S. *Laffey*, and U. S. S. *Blish* during Operation Crossroads. These records were the only ones available within the Marshall Islands area. The remaining sections in plate 78 and that given in plate 79*B* are based on observations taken aboard the Fish and Wildlife Service Motor Vessels *Hugh M. Smith* and *John R. Manning* by the Pacific Oceanic Fisheries Investigations of the U. S. Fish and Wildlife Service under the direction of Townsend Cromwell. Plate 78 shows two sections, at longitude 172° W., giving differences between February and July of 1950 at this location; other sections in plate 78 and the section in plate 79*B* give the differences for the same period at longitude 158° W.

Observations given in plate 79*A* and *D* were made from U. S. Navy ships on wartime missions. Plate 79*C* is based on observations made aboard the U. S. C. G. C. *Northwind* while returning from Operation Highjump in the Antarctic. Plate 79*E* and *F* is based on observations taken during the Scripps Institution–U. S. Navy Electronics Laboratory Mid-Pacific Expedition of 1950. Plate 79*G* and *H* is based on observations taken by U. S. Navy Electronics Laboratory personnel aboard the U. S. S. *Serrano*. In plate 79 the sections cross the currents diagonally as indicated by the longitude stations given on the plate.

Although internal waves introduce many irregularities into the depth of the thermocline and the isotherms, in general the depth of the thermocline decreases northward from about latitude 3° to latitude 5° N., reaches a minimum depth between latitudes 6° and 10° N., then increases in depth again to the north. To the south of the region of minimum thermocline depth, or current boundary zone, the Equatorial Countercurrent flows east: to the north the North Equatorial Current flows west. South of latitudes 3° to 5° N. the thermocline depth also decreases, but in this region of the South Equatorial Current the thermocline depths remain greater than in the boundary zone to the north. Marked differences are seen in the sections from west to east, particularly in the width of the Equatorial Countercurrent and in the thermocline depth in the current boundary zone. However, of particular interest to the geologist and biologist is the presence of temperatures inimical to the growth of coral reefs in the euphotic zone in the eastern Pacific and the absence of these cold temperatures in the euphotic zone in the western Pacific.

### TEMPERATURE DISTRIBUTION IN 1-DEGREE SQUARE SURROUNDING BIKINI ATOLL

Figures 98 and 99 are based on the 900-foot bathythermograph observations taken during Operation Crossroads. Figure 98 gives an average picture of the observations taken from May 8th to July 9th, and figure 99 is based on observations taken between July 20th and August 4th. It should be noted that the contour interval at the surface and at 200 feet is 0.2° F; at 300 and 400 feet it is 0.5° F, and at 600 and 800 feet it is 1.0° F. The temperature range within this area above the thermocline ranges from 1° F to 3° F, but below the thermocline it increases to 10° F. These charts are included to indicate the possible deviation from the average values of the isotherms in the horizontal charts (pls. 74, 75, 76) which can be expected for individual observations within a 1-degree square.

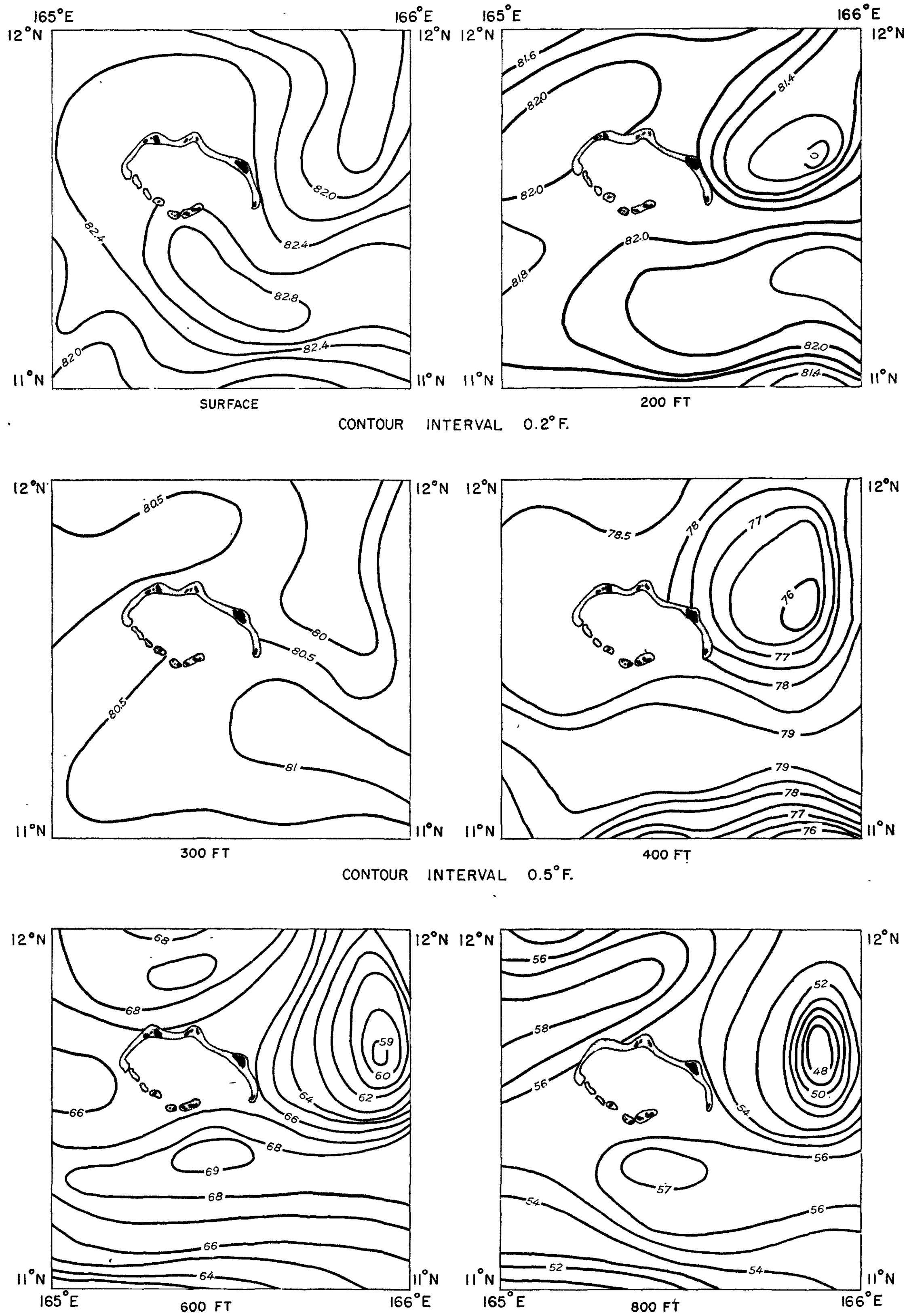


FIGURE 98.—Average temperature of water surrounding Bikini Atoll, May 8 to July 9, 1946, at the surface and at 200, 300, 400, 600, and 800 feet.

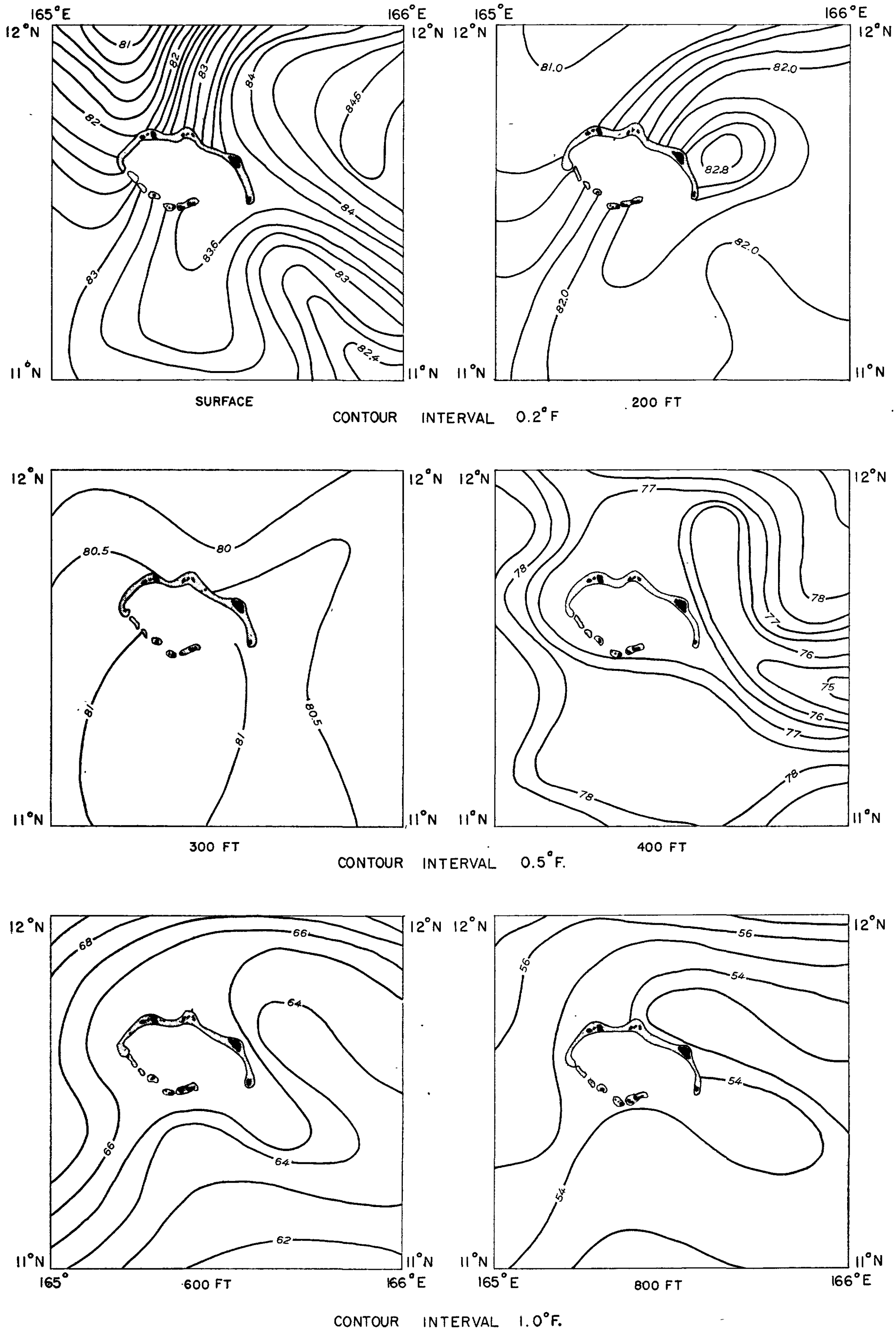


FIGURE 99.—Average temperature of water surrounding Bikini Atoll, July 20 to August 4, 1946, at the surface and at 200, 300, 400, 600, and 800 feet.

## LITERATURE CITED

Barnes, C. A., Bumpus, D. R., and Lyman, J., 1948, Ocean circulation in the Marshall Island area: Am. Geophys. Union Trans., v. 29, p. 871–876.

Cromwell, Townsend, 1951, Mid-Pacific oceanography, January through March 1950: U. S. Fish and Wildlife Service Special Scientific Report, Fisheries no. 54.

Mao, Han-Lee, and Yoshida, Kozo, 1954, Physical oceanography in the Marshall Islands area: U. S. Geol. Survey Professional Paper 260–R.

Sverdrup, H. U., Johnson, M. W., and Fleming, R. H., 1946, The oceans, their physics, chemistry, and general biology, 1,087 p., 7 charts, New York, Prentice Hall, Inc.